



1 AERO-MAP: A data compilation and modelling approach to 2 understand the fine and coarse mode aerosol composition

3 Natalie M. Mahowald¹, Longlei Li¹, Julius Vira², Marje Prank², Douglas S. Hamilton³, Hitoshi Matsui⁴, Ron L. Miller⁵,
4 Louis Lu¹, Ezgi Akyuz⁶, Daphne Meidan¹, Peter Hess⁷, Heikki Lihavainen⁸, Christine Wiedinmyer⁹, Jenny Hand¹⁰, Maria
5 Grazia Alaimo¹¹, Célia Alves¹², Andres Alastuey¹³, Paulo Artaxo¹⁴, Africa Barreto¹⁵, Francisco Barraza¹⁶, Silvia Becagli¹⁷,
6 Giulia Calzolai¹⁷, Shankarararman Chellam¹⁸, Ying Chen¹⁹, Patrick Chuang²⁰, David D. Cohen²¹, Cristina Colombi²²,
7 Evangelia Diapouli²³, Gaetano Dongarra¹¹, Konstantinos Eleftheriadis²³, Corinne Galy-Lacaux²⁴, Cassandra Gaston²⁵, Dario
8 Gomez²⁶, Yenny González Ramos^{27,15}, Hannele Hakola², Roy M. Harrison²⁸, Chris Heyes²⁹, Barak Herut^{30,31}, Philip
9 Hopke^{32,33}, Christoph Hüglin³⁴, Maria Kanakidou^{35,36,37}, Zsófia Kertesz³⁸, Zbiginiw Klimont²⁹, Katriina Kyllönen², Fabrice
10 Lambert^{39,40}, Xiaohong Liu⁴¹, Remi Losno⁴², Franco Lucarelli¹⁷, Willy Maenhaut⁴³, Beatrice Marticorena⁴⁴, Randall V.
11 Martin⁴⁵, Nikolaos Mihalopoulos^{35,46}, Yasser Morera-Gomez⁴⁷, Adina Paytan⁴⁸, Joseph Prospero²⁵, Sergio Rodríguez^{49,15},
12 Patricia Smichowski²⁶, Daniela Varrica¹¹, Brenna Walsh⁴⁵, Crystal Weagle⁴⁵, Xi Zhao⁴¹

13 ¹Department of Earth and Atmospheric Sciences, Cornell University, Ithaca, NY, 14853, USA

14 ²Finnish Meteorological Institute, Helsinki, Finland

15 ³ Department of Marine, Earth and Atmospheric Sciences, North Carolina State, Rayleigh, NC, USA

16 ⁴ Graduate School of Environmental Studies, Nagoya University, Nagoya, Japan 464-8601

17 ⁵ National Aeronautics and Space Administration, Goddard Institute for Space Studies, Columbia University, NY, NY
18 10025, USA

19 ⁶ Eurasia Institute of Earth Sciences, Istanbul Technical University, 34467 Istanbul, Turkey

20 ⁷ Department of Biological and Environmental Engineering, Cornell University, Ithaca NY, USA

21 ⁸ SIOS Knowledge Centre, Postboks 156, 9171 Longyearbyen, Norway

22 ⁹ Cooperative Institute for Research in Environmental Sciences at the University of Colorado Boulder, Boulder, CO, USA

23 ¹⁰ Cooperative Institute for Research in the Atmosphere, Colorado State University, Fort Collins, CO, USA,

24 ¹¹ Dip. Scienze della Terra e del Mare, University of Palermo, Italy

25 ¹² Centre for Environmental and Marine Studies (CESAM), Department of Environment, University of Aveiro, 3810-193,
26 Aveiro, Portugal

27 ¹³ Institute of Environmental Assessment and Water Research (IDAEA-CSIC), 08034, Barcelona, Spain

28 ¹⁴ Instituto de Física, Universidade de São Paulo, 05508-090, São Paulo, SP, Brazil

29 ¹⁵ Izaña Atmospheric Research Center (IARC), Agencia Estatal de Meteorología (AEMET), Santa Cruz de Tenerife, Spain

30 ¹⁶ Saw Science, Invercargill, New Zealand

31 ¹⁷ Department of Physics and Astronomy, Università di Firenze and INFN-Firenze, 50019 Sesto Fiorentino, Italy



- 32 ¹⁸ Department of Civil & Environmental Engineering, Texas A&M University, College Station, TX 77843-3136, USA
33 ¹⁹ Department of Environmental Science and Engineering, Fudan University Jiangwan Campus 2005 Songhu Road,
34 Shanghai, China
35 ²⁰ Earth & Planetary Sciences Department, Institute of Marine Sciences, University of California, Santa Cruz, CA, 95064 ,
36 USA.
37 ²¹ Australian Nuclear Science and Technology Organisation, Lucas Heights, NSW, Australia
38 ²² Environmental Monitoring Sector, Arpa Lombardia, Via Rosellini 17, 20124 Milan, Italy
39 ²³ Environmental Radioactivity & Aerosol Technology for Atmospheric & Climate impact Lab, INRaSTES, N.C.S.R.
40 Demokritos, 15341 Ag. Paraskevi, Attiki, Greece
41 ²⁴ Laboratoire d Aerologie, Universite de Toulouse, CNRS, Observatoire Midi Pyrenees, Toulouse, France
42 ²⁵ Rosenstiel School of Marine and Atmospheric Science, University of Miami, Miami, FL, 33149, US
43 ²⁶ Comision Nacional de Energia Atomica, Gerencia Química, Av. Gral Paz 1499, B1650KNA, San Martin, Buenos Aires,
44 Argentina
45 ²⁷ Scientific Department, CIMEL, Paris, France.
46 ²⁸ School of Geography, Earth and Environmental Sciences, University of Birmingham, Edgbaston, Birmingham B15 2TT,
47 United Kingdom
48 ²⁹ Energy, Climate and Environment Program, International Institute for Applied Systems Analysis, 2361 Laxenburg,
49 Austria
50 ³⁰ Israel Oceanographic & Limnological Research, Tel Shikmona, Haifa, 31080, Israel
51 ³¹ Department of Marine Sciences, University of Haifa, Haifa, 3103301, Israel
52 ³² Department of Chemical and Biomolecular Engineering, Clarkson University, Potsdam, NY, USA,
53 ³³ Department of Public Health Sciences, University of Rochester School of Medicine and Dentistry, Rochester, NY, USA,
54 ³⁴ Swiss Federal Laboratories for Materials Science and Technology(EMPA), CH-8600 Duebendorf, Switzerland
55 ³⁵ Environmental Chemical Processes Laboratory (ECPL), Department of Chemistry, University of Crete, Heraklion, Greece.
56 ³⁶ Center of Studies of Air quality and Climate Change, Institute for Chemical Engineering Sciences, Foundation for
57 Research and Technology Hellas, Patras, Greece.
58 ³⁷ Excellence Chair, Institute of Environmental Physics, University of Bremen, Bremen, Germany
59 ³⁸ HUN-REN Institute for Nuclear Research (ATOMKI), Debrecen, Hungary
60 ³⁹ Geography Institute, Pontificia Universidad Catolica de Chile, Santiago, 7820436, Chile
61 ⁴⁰ Center for Climate and Resilience Research, Santiago, Chile
62 ⁴¹ Department of Atmospheric Sciences, Texas A&M University, College Station, TX 77843, USA
63 ⁴² Institut de Physique du Globe de Paris, Universite de Paris, Paris, France
64 ⁴³ Department of Chemistry, Ghent University, Gent, Belgium
65 ⁴⁴ Laboratoire Interuniversitaire des Systemes Atmospheriques (LISA), Universites Paris Est-Paris Diderot-Paris 7, UMR
66 CNRS 7583, Creteil, France
67 ⁴⁵ Energy, Environmental and Chemical Engineering, Washington University, St. Louis, MO, USA.
68 ⁴⁶ Institute for Environmental Research and Sustainable Development, National Observatory of Athens, Pendeli, Greece
69 ⁴⁷ Universidad de Navarra, Instituto de Biodiversidad y Medioambiente BIOMA, Irunlarrea 1, 31008, Pamplona, España
70 ⁴⁸ Earth and Planetary Science, University of California, Santa Cruz, CA, USA
71 ⁴⁹ Consejo Superior de Investigaciones Científicas, IPNA CSIC, Tenerife, Canary Islands, Spain.
72



73
74 *Correspondence to:* Natalie M. Mahowald (mahowald@cornell.edu)

75 **Abstract.** Aerosol particles are an important part of the Earth system, but their concentrations are spatially and temporally
76 heterogeneous, as well as variable in size and composition. Aerosol particles can interact with incoming solar radiation and
77 outgoing long wave radiation, change cloud properties, affect photochemistry, impact surface air quality, and when
78 deposited impact surface albedo of snow and ice, and modulate carbon dioxide uptake by the land and ocean. High aerosol
79 concentrations at the surface represent an important public health hazard. There are substantial datasets describing aerosol
80 particles in the literature or in public health databases, but they have not been compiled for easy use by the climate and air
81 quality modelling community. Here we present a new compilation of PM_{2.5} and PM₁₀ aerosol observations including
82 composition, a methodology for comparing the datasets to model output, and show the implications of these results using one
83 model. Overall, most of the planet or even the land fraction does not have sufficient observations of surface concentrations,
84 and especially particle composition to understand the current distribution of aerosol particles. Most climate models exclude
85 10–30% of the aerosol particles in both PM_{2.5} and PM₁₀ size fractions across large swaths of the globe in their current
86 configurations, with ammonium nitrate and agricultural dust aerosol being the most important omitted aerosol types. The
87 dataset is available on Zenodo (<https://zenodo.org/records/10459654>, Mahowald et al., 2024).

88

89 **1 Introduction**

90 Recent Intergovernmental Panel on Climate Change (IPCC) reports and studies have highlighted the role of uncertainties in
91 human-induced changes to aerosol concentration and composition in the atmosphere in limiting our ability to project future
92 climate (IPCC, 2021; Gulev et al., 2021; Szopa et al., 2021). Aerosol particles are also a major contributor to air quality
93 problems, which reduce life expectancy and quality of life (Burnett et al. 2018). Aerosol particles are suspended liquids or
94 solids in the atmosphere originating from diverse sources and composed of a wide variety of chemicals (e.g., sea salts, dust,
95 sulfate, nitrate, black carbon, organic carbon). Aerosol particles interact with incoming solar radiation, outgoing long wave
96 radiation, change cloud properties and lifetimes, and modify atmospheric photochemistry (Mahowald et al., 2011;
97 Kanakidou et al., 2018; Bellouin et al., 2020). Once deposited on the surface, they can modify land and ocean
98 biogeochemistry, as well as the albedo of snow and ice surfaces (Mahowald et al., 2017; Hansen and Nazarenko, 2004,
99 Skiles et al., 2018). New satellite remote sensing measurements provide important information about temporal and spatial
100 distribution of aerosol particles, but challenges remain in quantifying the chemical composition of aerosol particles (Kahn et
101 al., 2005; Tanré et al., 1997; Remer et al., 2005). In addition, the AERONET surface remote sensing network provides some
102 information about loading, size and absorbing aerosol properties related to composition (Holben et al., 1991; Dubovik et al.,
103 2002; Schuster et al., 2016; Goncalves et al., 2023; Obiso et al., 2023). Both the magnitude of the effects, and sometimes



104 the sign of the aerosol effects are dependent on the composition and size of aerosol particles (Mahowald et al., 2011b, 2014a;
105 Bond et al., 2013; IPCC, 2021). In addition, one cannot understand the impact of humans on aerosol particles without
106 understanding the sources of aerosol particles, which is related to their chemical composition. Obtaining information about
107 the composition and size of aerosol particles in many cases requires in situ observations, which are limited in space and time
108 (Hand et al. 2017; Philip et al. 2017; Yang et al. 2018; Collaud Coen et al. 2020).

109 The climate and aerosol modelling community, especially under the auspices of AEROCOM, has compiled datasets and
110 organized comparison projects that have provided substantial information to improve aerosol models (Huneeus et al., 2011;
111 Textor and others, 2006; Dentener et al., 2006; Schulz et al., 2006; Gliß et al., 2021) or knowledge of the aerosol properties
112 like cloud condensation nuclei (Laj et al., 2020; Fanourgakis et al., 2019). However, most of these comparisons include data
113 only from North America and Europe (e.g., Szopa et al., 2021). In addition, previous compilation studies have focused
114 primarily on understanding fine aerosol particles (here defined as particle with a diameter less than 2.5 μm) and improving
115 model simulation of these aerosol particles, because of their importance for air quality, cloud interactions and short-wave
116 forcing (Collaud Coen et al., 2020; Bellouin et al., 2020; Fanourgakis et al., 2019). Coarse mode aerosol particles (defined
117 as those particles with a diameter larger than 2.5 μm) are important for long wave radiation interactions, cloud seeding and
118 for biogeochemistry, and these interactions have received less attention (Jensen and Lee, 2008; Mahowald et al., 2011;
119 Karydis et al., 2017; Chatziparaschos et al. 2023). In contrast to the many fine aerosol compilations and comparisons
120 (usually considering particles with diameter less than 2.5 μm or PM_{2.5}), there are fewer studies focusing on aerosol
121 compilations for both fine and coarse aerosol particles, and their comparison to models (Kok et al., 2014b; Albani et al.,
122 2014b; Huneeus et al., 2011; Gliß et al., 2021, Kok et al., 2021). Nonetheless, there are many observations of the coarse
123 particle mass included in the particles with diameter less than 10 μm (PM₁₀) (e.g Hand et al., 2017), and most climate models
124 include these aerosol particles (e.g. Huneeus et al., 2011). Compilations of in situ data are available for dust and iron aerosol
125 particles (Kok et al., 2014b; Albani et al., 2014b; Mahowald et al., 2009) and for sea salts (Gong et al., 1997). Other studies
126 have focused on the important topics of wet deposition (Vet et al., 2014) or trends in aerosol properties (e.g., AOD, surface
127 PM) (Mortier et al., 2020; Aas et al., 2019). Observations of PM₁₀ or coarse and fine aerosol particles are available for many
128 regions and individual sites (e.g., Malm et al., 2007; Hand et al., 2019; Maenhaut and Cafmeyer, 1998; Artaxo and
129 Maenhaut, 1990; McNeill et al., 2020) but have not previously been compiled into one database. For example, much of the
130 air quality data used for deducing health impacts of aerosol particles is not publicly and easily available in a format
131 appropriate for use in Earth system models (e.g., van Donkelaar et al., 2021, <https://www.who.int/data/gho/data/themes/air-pollution/who-air-quality-database>). Aerosol modelers need as much information as possible about the composition of the
132 aerosol particles. Thus, there is a need to compile both PM_{2.5} and PM₁₀ in situ concentration data into one database to make
133 it easy for modellers to compare model results with observations. One goal the aerosol community should work towards is
134 making aerosol measurement datasets publicly available, while acknowledging the principal investigators who produced
135 these datasets, which we hope this paper serves as a step towards achieving.
136



137 The current generation of Earth system models used for the IPCC simulations tends to include the dominant aerosol
138 particles (desert dust, sea spray, black carbon (BC), organic matter (OM) and sulfate) but not all aerosol particles. For
139 example, some Earth system models ignore ammonium nitrate aerosol particles although these are known to be important for
140 climate and biogeochemistry, and are impacted by human activities (Paulot et al. 2016; Adams et al., 1999; Thornhill et al.,
141 2020). In addition, some models focus only on fine mode OM and BC aerosol particles, although there is evidence for
142 coarse mode aerosol particles of both carbonaceous aerosol particles (Graham et al., 2003; Mahowald et al., 2005).
143 Agricultural or land use sources of dust are not included in most models, although they could represent 25% of the
144 anthropogenic sources (Ginoux et al., 2012), and significantly impact transported transhemispheric aerosol composition
145 (García et al., 2017). In addition, fugitive, combustion and industrial dust emissions have traditionally been ignored as well,
146 although emission datasets are available (Philip et al., 2017). In this study we use available observations to constrain a
147 model estimate of the total PM₁₀ and PM_{2.5}, and deduce the importance of these often-neglected aerosol particles. We
148 propose a methodology for constraining aerosol particles that are not directly measured (dust or sea salts) using their
149 elemental composition. Note that we exclude super coarse (>PM10) particles here because of the lack of available data,
150 although studies have suggested their importance for climate interactions (e.g. Adebyi et al., 2023).

151 Harmonizing models with different types of measurements is critical (Huang et al., 2019). Models operate with the
152 geometric or aerodynamic particle diameter, whereas in practise the measurements are done with a variety of particle
153 equivalent diameter, e.g., optical, volume equivalent, projected-area equivalent, aerodynamic diameter or electrical mobility
154 diameter, depending on the instrument used (Hinds, 1999; Reid et al., 2003; Rodríguez et al., 2012). In the inlets of the
155 samplers used for the mass-measurements and collection of PM_{2.5} and PM₁₀ particles for subsequent chemical analysis, such
156 size cut-off at 2.5 µm and 10 µm is defined in terms of aerodynamic diameter (i.e., geometric diametric weighed by the
157 particle density; Hinds, 1999). The sharpness of the cut-off of such inlets influences the PM_{2.5} and PM₁₀ mass concentration
158 (Hand et al., 2019; Wilson et al., 2012). The PM₁₀ size cut-off aerodynamic diameter is equivalent to PM_{6.3} geometric
159 diameter for spherical dust particles (Hinds, 1999; Rodríguez et al., 2012) and to PM_{6.9} in the case of dust aspherical particles
160 (Huang et al., 2021). Similarly, PM_{2.5} (aerodynamic diameter) is equivalent to PM_{1.6} (geometric diameter) for dust. We
161 consider the importance of this in global model simulations and comparisons to observations. Similar issues can occur for
162 PM_{2.5} sized particles, which we do not yet consider in this study. In addition, there are issues about the temporal changes in
163 aerosols. There have been substantial trends in emissions especially of anthropogenic aerosols over the last 40 years (Quass
164 et al., 2022; Bauer et al., 2022). For this first study we include all aerosol data available, spanning 1970s to 2020s. Future
165 studies will consider the temporal changes in the data in more detail.

166 For this study we focus on the following: a) compiling available PM_{2.5} and PM₁₀ aerosol data, including aerosol
167 composition into a new publicly available database for the modelling community (AEROMAP); b) presenting a
168 methodology to compare these observations to an Earth system model, which has extended the normal sources of aerosol



169 particles to include more types of aerosols such as agricultural dust, nitrates, etc.; c) identifying the measurement and
170 modelling gaps from this comparison. In this paper, we focus on the annual average distribution of aerosol particles and
171 some key chemical composition information. Future studies will focus on seasonal and daily scale variations and temporal
172 trends as well as trends in other chemicals or elements within the aerosols.

173 **2 Description of Methods**

174 **2.1 Observational data**

175 PM observations are made by multiple networks, or during specific field campaigns, and for different size cut-offs, with and
176 without a description of chemical composition. As expected, most of the observations are over North America or Europe,
177 with much of the rest of the land areas and most of the ocean much more poorly observed (Fig. 1; supplemental dataset 1).
178 For this study, we include both PM_{2.5} and PM₁₀ daily (or multiple day averages) data sets that were made available by the
179 investigators or are available from public web sites (Fig. 1; supplemental dataset 1). Some measurement sites measure PM_{2.5}
180 and coarse (PM_{2.5} to PM₁₀) aerosols. For those sites, we convert the latter to PM₁₀ for comparison. Some measurement sites
181 have only a few observations of composition or mass, while others have multiple years: we included less complete datasets
182 at sites in regions with limited data. The time period for different datasets is included in the supplemental information.

183 Detailed studies have shown that PM₁₀ and PM_{2.5} samplers can differ in the sharpness of their size cut-off (Hand et al.,
184 2019). As an example, comparisons between data from the U.S. Environmental Protection Agency (EPA) Federal Reference
185 Method sites and data from the Interagency Monitoring of Protected Visual Environments (IMPROVE) network show that
186 the coarse matter from collocated sites in both networks were offset by 28% (Hand et al., 2019). There was a bias when data
187 were compared (slope of 0.9), but the correlation coefficient was high (0.9) suggesting overall a good agreement. We focus
188 here on surface station measurements of PM₁₀ and PM_{2.5}, since our model and most models only consider mass up to PM₁₀.
189 For that reason, our model deposition is not directly comparable to observational bulk/total atmospheric deposition since
190 larger particles may dominate the deposition close to the source areas (Kok et al., 2017; Mahowald et al., 2014b; Neff et al.,
191 2013). Measuring absolute dry and wet deposition rates is also technically more challenging (especially dry deposition, since
192 the particles can be re-entrained into the atmosphere), but worthwhile (Heimbürger et al., 2012; Prospero et al., 1996). In
193 regions with little data (e.g., outside of North America and Europe) we include measurements of total suspended particulates
194 (TSP) with the PM₁₀, because of the lack of size-resolved data. Data from the Japanese air quality network use a different
195 inlet for the PM10 cutoff as well, which will include a slightly larger size fraction (<https://tenbou.nies.go.jp/download/>).

196 In addition to particulate matter in the PM₁₀ and PM_{2.5} size fractions, we also compile the following observations to compare
197 to the model: black carbon (BC), elemental carbon (EC), organic carbon (OC) (or particulate organic material, OM, that is



here considered to be 1.8 x OC in mass), sulfate, nitrate, aluminum, sodium and chloride. To include both BC (based on light absorption measurements) and EC (based on thermal oxidation induced combustion measurements) data are also a source of uncertainty, both are proxies of the soot combustion particles since they are based on different measurements techniques, and there is no accepted equivalence between them (Mbengue et al., 2021). Details on how the model is compared to data for different elements is in section 3.2.

For this paper, we focus on the annual means which are calculated for all values at each station that are above the detection limit and reported here. At some stations or times, concentrations can be below the detection limit, and excluding these data or time periods could bias our average values. We focus on the stations that have more than 50% of the data above the detection limit, and exclude other sites. For those included stations, if the values were reported as below the detection limit, we include in the average one-third of the minimum detection limit. The reported detection limits should bound the upper limit of aerosol mass and allow us to include sites, whose observations were otherwise too low to include, while reducing the potential biasing of our compilation towards higher values (doi: 10.5281/zenodo.10459654, Mahowald et al., 2024).

2.2 Model description

Simulations of aerosol particles were conducted using the aerosol parameterizations within the Community Atmosphere Model, version 6 (CAM6), the atmospheric component of the Community Earth System Model (CESM) developed at the National Center for Atmospheric Research (NCAR) (Hurrell et al., 2013; Scanza et al., 2015; Liu et al., 2012). The aerosol module in this version is closely related to the module used in the Energy Exascale Earth System Model (Golaz et al., 2019; Caldwell et al., 2019). Simulations were conducted at approximately $1^\circ \times 1^\circ$ horizontal resolution with 56 vertical layers for four years, with the last three years (2013-2015) used for the analysis (Computational and Information Systems Laboratory, 2019). The model simulates three-dimensional transport and wet and dry deposition for gases and aerosol particles based on MERRA2 winds (Gelaro et al., 2017).

The model included prognostic dust, sea salts, BC, OM, and sulfate aerosol particles in the default version, using a modal scheme based on monthly mean emissions for the year 2010 (Liu et al., 2012, 2016; Li et al., 2021). For this study, the coarse size mode (mode 3) was returned to the CAM5 size parameters (geometric standard deviation of 1.8) to better simulate coarse mode aerosol particles, and improve the dry deposition scheme and optics used in the model for simulating coarse mode aerosol particles like dust as described in Li et al. (2022b).

Desert dust is entrained into the atmosphere in dry, sparsely vegetated regions subject to strong winds. We use the Dust Entrainment and Deposition scheme (Zender et al., 2003) with the emitted size distribution given by the updated Brittle Fragmentation Theory (Kok et al., 2014b, a) with improved incorporation of aspherical particles for optics and deposition (Li



227 et al., 2022b; Huang et al., 2021; Kok et al., 2017). Fossil fuel and natural emissions of sulfate, OM, and BC follow the
228 Climate Model Intercomparison Project 6 emission scenarios for present day (Gidden et al., 2019).

229 **2.2.1 Modelling of additional aerosol sources and types**

230 The model was modified to allow the addition of several new aerosol particles based on codes with expanded dust speciation
231 (Li et al., 2022b) but here the extra dust tracers are used for the additional species as described below. The additional
232 sources of aerosol particles use the same optical properties as bulk dust for this sensitivity study. The following aerosol
233 particles were added, and the amount of emissions in each the PM_{2.5} and PM₁₀ sizes and contribution to surface concentration
234 and aerosol optical depth are shown in Table 1. In addition, some of the base case aerosol emissions were modified to match
235 observations, as discussed below.

236 Agricultural sources of dust are added to this version of the model using the same emission scheme as for natural sources
237 (Kok et al., 2014b, a; Li et al., 2022b), but applied to the crop area, and each region is tuned to have the percentage amount
238 of anthropogenic dust to match satellite based observations (Ginoux et al., 2012), except Australia, where other estimates
239 (Bullard et al., 2008; Mahowald et al., 2009; Webb and Pierre, 2018) suggest a lower amount (see Table S1 for comparisons,
240 based on Brodsky et al., 2023). Agricultural dust is separately considered by the model, so its importance can be isolated.

241 Coarse BC and O_< as well as fine and coarse ash from industrial sources were added. Emissions estimated from the GAIN
242 model are added to the model using the ECLIPSEV6_CLE base case (Klimont et al., 2017; Philip et al., 2017). Coarse BC
243 and OM from biomass burning were assumed to be 20% of the fine mode mass (Mahowald et al., 2005).

244 Primary biogenic particles are released from ecosystems either as integral particles, such as bacteria, pollen or spores, or as
245 accidentally entrained leaf pieces (Jaenicke, 2005; Mahowald et al., 2008; Despres et al., 2012; Burrows et al., 2009; Heald
246 and Spracklen, 2009). These sources are poorly observed or understood, and thus looking at coarse mode organic material in
247 this study could provide additional constraints on the budget. Assumptions about size are likely to be very important for the
248 resulting distribution and impacts (e.g., compare P budgets from assuming one size versus five different bins (Brahney et al.,
249 2015)). Four different types of primary biogenic particles were included: bacteria, spores and other miscellaneous emissions
250 (leaf bits, pollen, etc.) from land ecosystems, as well as a marine organic aerosol. Included bacteria sources were read in
251 from a monthly climatology (Burrows et al., 2009). Spore sources were calculated offline and read into the model based on
252 observed leaf area index, temperature, and a source parameterization (Janssen et al., 2020; Heald and Spracklen, 2009).
253 Other terrestrial emissions were estimated based on leaf area index following Mahowald et al. (2008). Marine organic
254 aerosol emissions were included based on the physically based scheme OCEANFILMS (Burrows et al. 2014). Marine
255 organics are externally mixed with sea spray, following Zhao et al. (2021). OCEANFILMS only estimates the fine mode



256 organic mass, and here we assume that the coarse mode marine organic mass equals 1% of the seaspray mass, (Gantt et al.,
257 2011). The assumptions about the mass and fraction in each size bin are shown in Table 1.

258 Ammonium nitrate aerosol particles are not included in the standard CAM6 nor in E3SM, but are thought to be important for
259 aerosol optical depth and surface concentrations (Paulot et al., 2016; Adams et al., 1999; Thornhill et al., 2020, Bauer et al.,
260 2007, 2016). Nitrate can also be taken up onto dust particles, for example, but that is ignored in this study (Dentener et al.,
261 1996). Ammonium nitrate aerosol particles require tropospheric chemistry interactions because the nitrogen based aerosol
262 particles interact with tropospheric photochemistry and the aerosol particles are in chemical equilibrium with the gas phase
263 (e.g. Nenes et al., 2021; Baker et al., 2021; Bauer et al., 2007; 2016), so simulations using the CAM-CHEM model with
264 tropospheric photochemistry are used covering the same time period (Vira et al., 2022). Simulations with chemistry were
265 conducted at $2^\circ \times 2^\circ$ resolution and are linearly interpolated to $1^\circ \times 1^\circ$ resolution used for the other modelled aerosol particles.
266 Sulfate in the CAM6 is assumed to be in the form of ammonium sulfate and the nitrate is assumed to be in the form of
267 ammonium nitrate for these studies, so as a rough approximation only the ammonium nitrate needs to be added to consider
268 nitrogen aerosol optical depth. While aerosol amounts are simulated, ammonium nitrate aerosol optical depth is not
269 calculated within the model but offline. The model does calculate sulfate aerosol optical depth, which has a roughly similar
270 increase in size with humidity, and similar optical properties as long as the nitrates and sulfates are in similar size fractions
271 (Paulot et al., 2016; Bellouin et al., 2020). Therefore the aerosol optical depth from ammonium nitrate (per unit mass) is
272 assumed to be proportional to the sulfate aerosol optical depth per unit mass in each grid box at each time interval. Detailed
273 comparison of the nitrate and ammonia aerosol particles, and other species was conducted in Vira et al. (2022). Overall, the
274 model can simulate some of the spatial distribution, but overestimates the nitrate aerosol amounts. This is also seen in Vira et
275 al. (2022), and as shown in Table 1, the calculated nitrate aerosol amounts are multiplied by 0.5 to best match the available
276 observations.

277 2.3 Model-observation comparison methodology

278 Comparisons of the observations to model concentrations were done using BC, OC, SO_4^{2-} , Al, NO_3^- , NH_4^+ , Na, and Cl
279 composition measurements. Some of these elements/compounds map directly onto model constituents (BC, OC, SO_4^{2-} , NO_3^- ,
280 , and NH_4^+), while others serve as proxies for modelled constituents (Al for dust and industrial ash, Na and Cl for sea salts, S
281 for sulfate, etc.). We use non-sea-salt sulfate in ocean regions for estimating sulfate. Some observing networks like
282 IMPROVE use a composite of elements to deduce dust amounts (e.g., Hand et al., 2017). We do not choose to do this for
283 two reasons: first at some sites not all the elements are available, and secondly because these elements are not only from
284 desert dust, but also from industrial sources, so we explicitly include industrial ash sources and Al in those sources to
285 compare. Note that model values come from the midpoint of the bottom level of the model (~30 m) while the observations
286 are usually taken at 2 or 10 m high. Modelled values of PM content, which assume dry particles, are used, while gravimetric



287 measurements in some networks are equilibrated at 50% relative humidity, thus 5-25% of the mass of measured PM can be
288 water (Prank et al., 2016; Burgos et al., 2020).

289 For the most part, we use model output for which there is a one to one relationship with what is being measured (BC, sulfate,
290 etc). However, for dust this is not straightforward, as dust is composed of multiple elements. Here we use Al as a proxy for
291 dust, as it is relatively constant (~7%) in dust (as opposed to Ca, which varies highly, or Fe which varies moderately) (Zhang
292 et al., 2015). Al sources are primarily from dust, agricultural dust, road dust and industrial ash emissions; we ignore minor
293 emissions from volcanoes, marine sea spray and primary biogenics for this study (Mahowald et al., 2018). Assumptions
294 about the model composition and how they are compared to observations are shown in Table S2. Since we compare the sea
295 salt variable to both Na and Cl (if Na is not available), we show the conversion of Cl to Na for sea salt calculations, and
296 other assumptions for converting observations to be consistent with each other in Table S3. For example, OM is assumed to
297 be 1.8 times OC.

298 Previous studies have pointed out that PM₁₀ observations of dust represent an approximate cut-off of the aerodynamic
299 diameter of 10 µm, which could be converted within the model to a 6.9 µm geometric diameter cut-off assuming spheroids,
300 like dust (Huang et al., 2021). Using standard relationships between the modal aerosol particles used in the CAM6 (Liu et
301 al., 2016) and the fraction of the aerosol particles below 6.9 µm (Seinfeld and Pandis, 2006) (here referred to as PM_{6.9}), a
302 new diagnostic was added to the model, which shows that in regions with substantial coarse aerosol particles like dust, there
303 can be a difference of about 30%, while in most places the differences are less than 5% (Fig. S1). These assumptions are less
304 true for coarse particles like sea salts, but the differences are small in sea salt dominated regions (Fig. S1). For this study we
305 use PM_{6.9} from the model. Note that the inlet size discrimination for PM_{2.5} measurements are also not a step function and also
306 this might impact the comparisons for PM_{2.5}.

307 For ease of viewing the data in this paper in the densely sampled regions, observational records from different sites were
308 combined into a mean within a grid cell that is two times the model resolution, or approximately 2° x 2°. This process
309 averages the observations over a spatial scale appropriate for comparison with the chemistry model (Schutgens et al., 2016).
310 We provide both the annual average data at each site as well as the averaged data (with the modelled data at doi:
311 10.5281/zenodo.10459654, Mahowald et al., 2024).

312 Notice that we include both urban regions and rural or remote sites into the same dataset. Some of the data is not resolved in
313 location better than 0.25 degrees, so that the coordinates of the locations here provided with the gridded data should not
314 necessarily be used for finer resolution studies. Because of the importance and size of megacities crossing multiple grid
315 boxes including available data are more representative than excluding polluted regions for air quality and climate studies, but
316 each application should make appropriate choices, and studies show expected differences between urban and rural
317 concentrations and trends (e.g., Hand et al., 2019).



318 **3 Results**

319 **3.1 AEROMAP observational data set**

320 First, we assess the amount of data and the number of stations within each $\sim 2^\circ \times 2^\circ$ gridded area (Fig. 1). The observational
321 dataset provides coverage predominately over North America and Europe for PM_{2.5} and PM₁₀, as noted by previous studies
322 (e.g., Szopa et al., 2021), but in addition we provide here a synthesis of more air quality data in other regions, especially Asia
323 (Fig. 1). This data set comprises most of the individual observations (at daily or higher time periods) of total PM_{2.5} (Fig. 1a,
324 1e: blue bars) and most of the observing stations (Fig. 1e and blue line). Approximately 15,000 stations and over 20 million
325 observations are included in this compilation as annual averages.

326 Notice that there are two to three orders of magnitude more daily observations for the total mass (PM) of aerosol particles
327 compared to information about the composition of aerosol particles (Fig. 1e, which is shown also by contrasting the spatial
328 distribution of measurements between PM_{2.5} and measured amounts of OM (Fig. 1a versus 1b), as well as a large difference
329 between the number of stations measuring the total mass versus the speciated aerosol particles like OM (Fig. 1c versus 1d).
330 While this dataset presents a huge increase in the amount of data available to the aerosol modelling community, still most of
331 the total PM_{2.5} or PM₁₀ data are clustered over a few regions, and there is little composition information over most of the
332 globe (Fig. 1).

333 This dataset is presented as an annual mean, but the data span 1986 to 2023 (Fig. 1f). Over this time period there are
334 statistically significant trends in different regions (Quass et al., 2022; Bauer et al., 2022). For this dataset we choose to
335 present all the data averaged, but in future studies there will be datasets of seasonality and interannual variability of aerosols
336 as available. Note that the model uses emission estimates for 2010, and meteorology for 2013-2015, so that there could be
337 differences in the model-data comparison because of the time period discrepancies.

338 **3.2 PM_{2.5} model-data comparison**

339 Modelled concentrations of PM_{2.5} are more often compared against observations than for PM₁₀ or other size fractions, and
340 comprise an important portion of the particulate matter associated with human activities. Therefore, we describe first the
341 observational synthesis and comparison to model results for PM_{2.5}. Because the high number of observations in some parts of
342 the world would make the figures unreadable, the observations are gridded onto an approximately $2^\circ \times 2^\circ$ grid for
343 comparisons with the model (Fig. 2a). As expected, in the model the highest concentrations are over the desert dust regions,
344 such as North Africa, and over heavily industrialized regions in Asia. For the heavily industrialized regions in Asia, these
345 high values are consistent with the observations, but the regions in North Africa with the highest modelled values do not
346 have similar observational validation for high concentration values due to a lack of data (Fig. 2a).



347 Overall, the model is able to simulate much of the spatial variability in PM_{2.5} over two orders of magnitude (Fig. 2a and 2c),
348 however there is an overestimate in the PM_{2.5} over India and China (Fig. 2b). These discrepancies over India and China could
349 be due to errors in the input emissions datasets or the aerosol transport modelling, or to differences in the time periods
350 covered: the observations are more recent while the assumptions for the emissions are for the year 2010. There could also be
351 methodological and analytical differences due to which group or network did the observations or the exact locations of the
352 different monitors. Much of the data in those regions are not usually included in compilations of data, so the fact that
353 previous model studies have not been able to assess emission datasets in these regions could explain this discrepancy.
354 Comparison between different observations in some cities (Fig. 3) shows that in these grid boxes there can be very large
355 differences (~factor of 3) between the annually averaged values reported at nearby stations within 1° distance radially, and
356 that the AirNow measurements (<https://www.airnow.gov/international/us-embassies-and-consulates/> on the US
357 embassies) tend to be higher than those reported from government air quality networks. The sites compared are in large cities
358 and thus are likely to have strong local sources and intense gradients in pollutants. For now, we keep in mind this large
359 difference, but continue to use the observations. As indicated below, in these regions we do not have measurements of
360 composition so we do not know which constituents are poorly simulated in our emissions or transport modelling. More
361 statistics describing the model data comparisons are shown in Table S4.

362 The scatterplots show the comparisons of the model to the observations using the gridded data (Fig. 2c) and all original data
363 (Fig. 2d), and the correlation coefficients are slightly better using the original data (Fig. 2d) (0.78versus 0.69 for the gridded
364 data). Notice that most of the data in the Asian region (blue plusses) show the highest model bias.

365 Next, we consider the composition of the PM_{2.5} aerosol in the model versus the observations, starting with the aerosol
366 components in the default version of the model. Sulfate aerosol particles tend to be overestimated in the model in North
367 America, but not over Europe and other regions (Fig. 4a and b). Previous studies have compared SO₄²⁻ aerosol observations
368 to simulations and have not noted this bias (e.g., Barrie et al., 2001; Aas et al., 2019) but this bias was seen in this model
369 (Liu et al., 2012; Yang et al., 2018). BC comparisons suggest the model results are roughly able ($r=0.25$) to capture the
370 spatial dynamics of this aerosol across more than 2 orders of magnitude (Fig. 4c and d). This is similar to previous model
371 intercomparisons (Koch et al., 2009; Bond et al., 2004, 2013; Liu et al., 2012, 2016). Simulations of OM in the default
372 model suggest that the model has difficulty in simulating all the variability in OM. Correctly modelling organic material is
373 very difficult both due to the sparsity of data for comparison, as well as the existence and importance of OM in both primary
374 and secondary aerosol particles (Heald et al., 2010; Kanakidou et al., 2005; Olson et al., 1997; Tsigaridis et al., 2014), and
375 previous studies with this model have noted an overestimate in comparison with surface observations (Liu et al., 2012). In
376 our study we include primary biogenic aerosol particles, which are usually not included in model studies (Mahowald et al.,
377 2011, 2008; Jaenicke, 2005; Heald and Spracklen, 2009; Burrows et al., 2009; Myriokefalitakis et al., 2016), but these are a



378 very small part of the PM_{2.5} and occur mostly in the coarse fraction (Table 1) and thus are not causing the bias, which must
379 be due to biomass burning and/or industrial emissions.

380 As a proxy for sea salts, we use the elemental data of the major components, Na and Cl, and there the model tends to be too
381 high at low Na and too low at high Na in North America, where much of the data are available (Fig. 4g and h), which has
382 been seen previously with this model (Liu et al., 2012). Notice that we do not include industrial emissions of Na or Cl as
383 they have not been spatially estimated. As a proxy for dust, we use Al amounts (Fig. 4i and j), which globally and over dust
384 regions are dominated by dust, although there are few observational datasets in high dust regions. The comparisons suggest
385 the model is able to simulate dust across 4 orders of magnitude, similar to previous studies (Liu et al., 2012; Albani et al.,
386 2014a; Li et al., 2022b; Huneeus et al., 2011) although there is a tendency for a high bias in the models over low dust regions
387 and a low bias in high dust regions, similar to sea salts (Fig. 4i and 4.j).

388 Next, we consider the nitrogen aerosol ammonium nitrate which requires complicated gas-aerosol phase equilibrium to
389 correctly simulate (e.g., Bauer et al., 2007; Thornhill et al., 2021; Adams et al., 2001; Regayre et al., 2018; Seinfeld and
390 Pandis, 1998). To summarize these complicated interactions, because SO₄²⁻ is a stronger acid than NO₃⁻ in the atmosphere,
391 the basic NH₄⁺ is preferentially found with SO₄²⁻. Thus NO₃⁻ aerosol particles will only form if there is sufficient NH₄⁺ left
392 over, therefore the ratio of NO₃⁻ to NH₄⁺ can vary. As described in the methods, to include these aerosol particles we used
393 simulations from a different version of the same model which include chemistry (Vira et al., 2022), and a more process-
394 based source of ammonia (Vira et al., 2020) since the default CESM2 version used here for most aerosol particles does not
395 include chemistry. Note that even in the chemistry version of the model for CESM2 the complicated gas-aerosol phase
396 equilibrium is not included, which causes errors in the simulation of the amounts of nitrogen aerosol (e.g., Bauer et al., 2007;
397 Thornhill et al., 2021; Adams et al., 2001; Regayre et al., 2018; Nenes et al., 2021); thus while the NH₃ emission scheme
398 used in this model is state-of-the-art, the lack of an adequate gas-aerosol phase separation may lead to biases as discussed in
399 Vira et al. (2022). NO₃⁻ aerosol particles compared against available observations show that over 2 orders of magnitude, the
400 model results are able to simulate the spatial variability (Fig. 4k and l). Note that here, we have multiplied the simulations by
401 a factor 0.5 in order to achieve a good mean comparison, as indicated by Vira et al. (2022). In addition, NH₄⁺ results show
402 the importance of NH₄⁺ over agricultural regions especially (e.g., Vira et al., 2022), and that the NH₄⁺ in the simulation used
403 here compares well to available observations (Fig. 4m and n; Vira et al., 2022).

404 3.3 PM₁₀ model-data comparison

405 PM₁₀ used to be the standard air quality measurement until more studies showed that smaller particles (PM_{2.5} or PM₁) were
406 more relevant for health impacts (e.g., <https://www.epa.gov/pm-pollution/timeline-particulate-matter-pm-national-ambient-air-quality-standards-naaqs>, accessed October 4, 2023). However, there are still many PM₁₀ measurements routinely made
407 (Fig 1d; Fig. 5a). As discussed in the methods, what is described as measurements of PM₁₀ (aerodynamic diameter) is
408



probably closer to PM_{6.9} (geometric diameter) as simulated in models (Huang et al., 2021), so here we use the PM_{6.9} fraction as calculated in the model to compare to PM₁₀ observations (Fig. S1 shows the fraction of PM₁₀ that is PM_{6.9}: this is only important in regions with substantial coarse mode emissions like desert dust source regions. For marine coarse aerosols like sea salt, the distinction between geometric and aerodynamic diameter may be smaller.). The model is able to simulate PM₁₀ concentrations across 2 orders of magnitude with some skill (Fig. 5a, c and d), although the region of East Asia, especially China and India are overestimated in the model similar to the PM_{2.5} (Fig. 3a, c and d). Gridding the data before comparing to the model results in a lower correlation across space than including all data (fig 5c vs. d), suggesting the existence of significant sub-grid variability and that some oversampled regions (e.g., European or North American cities) may be better simulated by emissions or transport models. Again we are including new data in this study that have previously not been used, and the discussion in the PM_{2.5} section is appropriate here (although we do not have AirNow measurements to compare against in the PM₁₀ size) for both the variability with grid cells as well as the potential for model and data errors. PM₁₀ aerosol particles have a shorter lifetime (Textor et al., 2006; Mahowald et al., 2011), allowing for more variability within a grid cell. More statistical comparisons are shown in Table S5.

There are fewer comparisons with PM₁₀ composition data available in the literature: usually only sea salts and dust are compared to observations which include the coarse mode (Gong et al., 2003; Ginoux et al., 2001; Albani et al., 2014b; Mahowald et al., 2006). Comparisons for SO₄²⁻ (Fig. 6a and b.) suggest that within a large range the model does a good job of simulating the available observations. Similarly, for BC, the PM₁₀ simulation captures the range of values, with less spread than SO₄²⁻ (Fig. 6c and d in contrast to a and b). Note that unlike many studies we include BC in the PM10 mode, since observations show that there is some contribution of BC to PM10 (compare figure 6c versus 4c). The model simulations for OM include primary biogenic particles and the limited available observations do not support larger sources of OM in the PM₁₀ than included here (as suggested in e.g., Jaenicke, 2005): indeed the model may be overestimating the OM in PM10. Similarly, the limited Na and Cl (proxy for sea salt) data suggest the model in some places may overestimate Na even over continents (Fig. 6g and h), as discussed in the PM_{2.5} section, as was seen previously (Liu et al., 2012). Comparisons with Al (proxy for dust) show that the mean is well simulated, but there are regions with poor agreement, consistent with previous studies with this model (Li et al., 2022b; Kok et al., 2014b; Albani et al., 2014a; Matsui and Mahowald, 2017; Zhao et al., 2022), and indeed across most dust models (Huneeus et al., 2011).

For the NO₃⁻ in aerosol particles, similar to the PM_{2.5} size, the particles were multiplied by 0.5 to better match the observations following Vira et al. (2022) (Fig 6k and l). The model simulations suggest too high values in high NO₃⁻ areas, and too low in low NO₃⁻ regions (Fig. 6k and l). NH₄⁺ shows a slightly better comparison to the limited available data (Fig. 6m and n) as seen in Vira et al. (2022). Note that as discussed earlier, the model does not include other forms of nitrate aerosols which may be important, such as the uptake of nitrate onto dust aerosols (Dentener et al., 1996; Xu and Penner, 2012;



443

444 **3.4 Data and model coverage**

445 The compilation shown here is the most comprehensive currently available for total mass and composition of in situ
446 concentration data, and yet it highlights the lack of sufficient data to constrain the current distribution of aerosol particles and
447 their composition (Fig. 7a and b). Only 3% of the grid boxes ($2^\circ \times 2^\circ$) have PM_{2.5} data (about 10% of land grid boxes), and
448 only 0.3% has sufficient data to constrain most of the composition (defined as having 90% of the variables considered here:
449 total mass, SO₄²⁻, BC, OM, Na or Cl, Al or dust, NO₃⁻ and NH₄⁺). There are even less data available to characterize PM₁₀,
450 which is less important for air quality and aerosol-cloud interactions but more important for aerosol-biogeochemistry
451 interactions and long wave interactions (Mahowald et al., 2011; Li et al., 2022a; Lim et al., 2012; Kanakidou et al., 2018).
452 Because of the high spatial and temporal variability and the lack of satellite or other remote sensing data to characterize the
453 type of aerosol, this lack of data is a severe handicap in constraining aerosol radiative forcing uncertainties and other impacts
454 of aerosol particles in the climate system.

455 In this simulation, we included several new aerosol sources and types that are not in the default model to investigate their
456 importance. For the CESM this simulation includes agricultural dust, nitrogen aerosol particles and several other sources
457 (see Table 1). As shown in Fig. 8, the default aerosol particles are the dominant aerosol particles over most of the planet, but
458 in many regions for both PM_{2.5} and PM₁₀, the default aerosol scheme includes less than 30% of the aerosol particles (Fig. 8a
459 and c), with substantial contributions from the new added aerosol particles (Fig. 8b and d), especially nitrogen aerosol
460 particles and agricultural dust. Many Earth system or climate models such as the CESM2 do not include nitrogen aerosol
461 particles (NO₃⁻ and NH₄⁺), because of the substantial complexity and computation load of chemistry and gas-aerosol
462 equilibrium (Bauer et al., 2007; Thornhill et al., 2021; Adams et al., 2001; Regayre et al., 2018)). Previous studies have
463 highlighted the importance of nitrogen aerosol particles for climate, air quality and ecosystem impacts (e.g., Adams et al.,
464 2001; Bauer et al., 2007, 2016; Kanakidou et al., 2016; Baker et al., 2021). Changes in nitrogen aerosol emissions are likely
465 to follow different future trajectories than SO₄²⁻, BC or OC, whose anthropogenic sources are mostly fossil fuel derived and
466 should decrease in the future as renewable energy resources expand (Gidden et al., 2019). Nitrogen aerosol particles have
467 substantial sources from agriculture, which is likely to stay constant or expand (Gidden et al., 2019; Klimont et al., 2017;
468 Bauer et al., 2016). This suggests there could be a substantial bias in both historical and future aerosol forcings due to the
469 lack of inclusion of these important sources (e.g., Bauer et al., 2007; Thornhill et al., 2021; Adams et al., 2001; Regayre et
470 al., 2018).



- 471 **4. Data availability:** The data compiled here is available as a csv table with citations as well as gridded datasets with the
472 modelled data in netcdf format at <https://zenodo.org/records/10459654>, Mahowald et al., 2024.

473 **5. Code availability:** The model used here is a version of the Community Earth System Model, and the modifications and
474 input files to that code are available at <https://zenodo.org/records/10459654>, Mahowald et al., 2024.

475

5. Conclusions

476 In this study, we present a new aerosol compilation (AERO-MAP) specifically designed for evaluating Earth system and air
477 quality models. This annual averaged dataset includes both total mass and composition, where available, including 12,000
478 station datasets and over 10 million daily averaged measurements. Here we expand beyond the usual biased coverage of
479 only North America and Europe to present a more global data view for both PM_{2.5} and PM₁₀ (Fig. 1). Unfortunately, there
480 are still very limited data characterizing both the surface concentration and composition of aerosol particles (Fig. 7). While
481 satellite remote sensing can indicate the total atmospheric loading, it cannot yet provide substantial information about the
482 size or composition of aerosol particles (Kahn et al., 2005; Tanré et al., 1997; Remer et al., 2005). Surface based remote
483 sensing may provide more information about size and absorption properties (Holben et al., 1991; Dubovik et al., 2002;
484 Schuster et al., 2016; Goncalves et al., 2023; Obiso et al., 2023). But knowing the size and the composition, which is key to
485 their impacts on air quality and climate (Mahowald et al., 2011) as well as their potential for future change (Gidden et al.,
486 2019) is important. We also present a methodology to use this dataset to evaluate both mass and composition for
487 intercomparison projects and improvements in air quality and Earth system models. Future studies will use this compiled
488 dataset for more detailed studies including temporal variability of different compositions. The fidelity of the annual means
489 provided by this study will depend upon the ability of the measurement networks to capture the observed multi-decadal
490 increases and decreases of emission that vary between source regions and sectors (Quaas et al., 2022).

491 This study also highlights the importance of including all aerosol components into the models, and shows that in the
492 CESM2, in many places there is between 10-60% of the aerosol particulate mass missing, largely due to lack of the nitrogen
493 aerosol particles (Paulot et al. 2016; Adams et al., 1999; Thornhill et al., 2020) and the poorly understood agricultural dust
494 aerosol particles (e.g., Ginoux et al., 2012). Because these aerosol particles are largely driven by agricultural sources and not
495 fossil fuels, their concentrations will be hardly impacted by the transition to renewable energy and may increase if
496 agricultural production expands with population. Therefore, these aerosol particles represent important air quality and
497 climate impacts that should be represented more accurately in future studies.

498 **Author contributions:** NMM designed and oversaw the implementation of the approach with the advice of HL, CW, RVM
499 and JL, and wrote the first draft of the manuscript. JV, PH, LLi, ZK, CD, SR, TB and DH assisted in the version of the
500 model and emission datasets used. EA, DM, HM and LLu authors assisted in the compilation and conversion of the data,



501 CH, ZK1 contributed emission datasets, XL and XZ contributed model code, MGA, CA, AA, PA, AB, FB, SB, GC, SC, YC,
502 PC, DC, CC, ED, GD, KE, CG-L, CG, DG, YGR, HH, RH, CH, BH, PH, CH, MK, ZKe, KK, FL, XL, RL, RL, WM, BM,
503 RM, NM, YM-G, AP, JP, SR, PS, DV, BW authors contributed data. All authors edited the manuscript.

504 **Competing interests:** The authors declare that they have no conflict of interest.

505 **Acknowledgments**

506 NMM and LL would like to acknowledge support from DOE (DE-SC0021302), as well as from the many freely available
507 air quality websites acknowledged in the paper. FB and FL would like to acknowledge support from the Ministerio del
508 Medio Ambiente de Chile (<https://mma.gob.cl>) and Fondecyt 1231682. SC is grateful for financial support from the Texas
509 Air Research Center and the Texas Commission on Environmental Quality. PA acknowledges funding from Fundação de
510 Amparo à Pesquisa do Estado de São Paulo (FAPESP), grants number 2017-17047-0 and 2023/04358-9. RVM
511 acknowledges funding from NSF Grant 2020673. MK and NM acknowledge support by Greece and the European Union
512 (European Regional Development Fund) via the project PANhellenic infrastructure for Atmospheric Composition and
513 climatE chAnGe (PANACEA, MIS 5021516). CGL and BM acknowledge support of CNRS, IRD and ACTRIS-France to the
514 International Network to study Atmospheric Deposition and Atmospheric chemistry in AFrica programe (INDAAF). HM
515 acknowledges support by the MEXT/JSPS KAKENHI Grant Numbers JP19H05699, JP19KK0265, JP20H00196,
516 JP20H00638, JP22H03722, JP22F22092, JP23H00515, JP23H00523, and JP23K18519, the MEXT Arctic Challenge for
517 Sustainability phase II (ArCS II; JPMXD1420318865) project, and by the Environment Research and Technology
518 Development Fund 2–2301 (JPMEERF20232001) of the Environmental Restoration and Conservation Agency. RLM
519 acknowledges support from the NASA Modeling, Analysis and Prediction Program. We acknowledge contributions from
520 Sagar Rathod, Tami Bond, Giles Bergametti, Javier Miranda Martin del Campo, ,and Xavier Querol. The support to CESAM
521 by FCT/MCTES (UIDP/50017/2020+UIDB/50017/2020+ LA/P/0094/2020) is also acknowledged.

522
523

524 **References**

525 Aas, W., Mortier, A., Bowersox, V., Cherian, R., Faluvegi, G., Fagerli, H., Hand, J., Klimont, Z., Galy-Lacaux, C.,
526 Lehmann, C. M. B., Myhre, C. L., Myhre, G., Olivié, D., Sato, K., Quaas, J., Rao, P. S. P., Schulz, M., Shindell, D.,



- 527 Skeie, R. B., Stein, A., Takemura, T., Tsyro, S., Vet, R., and Xu, X.: Global and regional trends of atmospheric
528 sulfur, *Sci Rep*, 9, <https://doi.org/10.1038/s41598-018-37304-0>, 2019.
- 529 Adams, P., Seinfeld, J., and Koch, D.: Global concentrations of tropospheric sulfate, nitrate and ammonium aerosol
530 simulated in a general circulation model, *J. Geophysical Research*, 104, 13791–13823, 1999.
- 531 Adams, P., Seinfeld, J., Koch, D., Mickley, L., and Jacob, D.: General circulation model assessment of direct radiative
532 forcing by sulfate-nitrate-ammonium-water inorganic aerosol system, *J Geophys Res*, 106, 1097–1111, 2001.
- 533 Adebiyi, A., Kok, J. F., Murray, B. J., Ryder, C. L., Stuut, J.-B. W., Kahn, R. A., Knippertz, P., Formenti, P., Mahowald, N.
534 M., Pérez García-Pando, C., Klose, M., Ansmann, A., Samset, B. H., Ito, A., Balkanski, Y., Di Biagio, C.,
535 Romanias, M. N., Huang, Y., and Meng, J.: A review of coarse mineral dust in the Earth system, *Aeolian Res*, 60,
536 100849, <https://doi.org/10.1016/j.aeolia.2022.100849>, 2023.
- 537 Alastuey, A., Querol, X., Aas, W., Lucarelli, F., Pérez, N., Moreno, T., Cavalli, F., Areskoug, H., Balan, V., Catrambone,
538 M., Ceburnis, D., Cerro, J. C., Conil, S., Gevorgyan, L., Hueglin, C., Imre, K., Jaffrezo, J. L., Leeson, S. R.,
539 Mihalopoulos, N., Mitosinkova, M., O'Dowd, C. D., Pey, J., Putaud, J. P., Riffault, V., Ripoll, A., Sciare, J.,
540 Sellegri, K., Spindler, G., and Yttri, K. E.: Geochemistry of PM10 over Europe during the EMEP intensive
541 measurement periods in summer 2012 and winter 2013, *Atmos Chem Phys*, 16, 6107–6129,
542 <https://doi.org/10.5194/acp-16-6107-2016>, 2016.
- 543 Albani, S., Mahowald, N. M., Perry, A. T., Scanza, R. A., Zender, C. S., Heavens, N. G., Maggi, V., Kok, J. F., and Otto-
544 Bliesner, B. L.: Improved dust representation in the Community Atmosphere Model, *J Adv Model Earth Syst*, 6,
545 541–570, <https://doi.org/10.1002/2013MS000279>, 2014a.
- 546 Albani, S., Mahowald, N., Perry, A., Scanza, R., Zender, C., and Flanner, M. G.: Improved representation of dust size and
547 optics in the CESM, *Journal of Advances in Modeling of Earth Systems*, 6, doi:10.1002/2013MS000279, 2014b.
- 548 Almeida, S. M., Pio, C. A., Freitas, M. C., Reis, M. A., and Trancoso, M. A.: Source apportionment of fine and coarse
549 particulate matter in a sub-urban area at the Western European Coast, *Atmos Environ*, 39, 3127–3138,
550 <https://doi.org/10.1016/j.atmosenv.2005.01.048>, 2005.
- 551 Amato, F., Alastuey, A., Karanasiou, A., Lucarelli, F., Nava, S., Calzolai, G., Severi, M., Becagli, S., Gianelle, V. L., Colombi,
552 C., Alves, C., Custódio, D., Nunes, T., Cerqueira, M., Pio, C., Eleftheriadis, K., Diapouli, E., Reche, C., Minguillón,
553 M. C., Manousakas, M. I., Maggos, T., Vratolis, S., Harrison, R. M., and Querol, X.: AIRUSE-LIFE+: A harmonized
554 PM speciation and source apportionment in five southern European cities, *Atmos Chem Phys*, 16, 3289–3309,
555 <https://doi.org/10.5194/acp-16-3289-2016>, 2016.
- 556 Andreae, T. W., Andreae, M. O., Ichoku, C., Maenhaut, W., Cafmeyer, J., Karnieli, A., and Orlovsky, L.: Light scattering by
557 dust and anthropogenic aerosol at a remote site in the Negev desert, Israel, *Journal Geophysical Research*, 107,
558 <https://doi.org/10.1029/2001JD900252>, 2002.
- 559 Arimoto, R., Duce, R. A., Ray, B. J., and Tomza, U.: Dry deposition of trace elements to the western North Atlantic, *Global*
560 *Biogeochem Cycles*, 17, <https://doi.org/10.1029/2001GB001406>, 2003.



- 561 Artaxo, P. and Maenhaut, W.: Aerosol characteristics and sources for the Amazon Basin during the west season, *J Geophys*
562 *Res*, 95, 16971–16985, 1990.
- 563 Artaxo, P., Martins, J. V., Yamasoe, M. A., Procopio, A. S., Pauliquevis, T. M., Andrae, M. O., Guyon, P., Gatti, L. V., and
564 Leal, A. M. C.: Physical and chemical properties of aerosol particles in the wet and dry seasons in Rondonia,
565 Amazonia, *J Geophys Res*, 107, 8081, doi: 10.1029/2001JD0000666, 2002.
- 566 Baker, A.R., Kanakidou, M., Nenes, A., Myriokefalitakis, S., Croot, P. L., Duce, R.A., Yuan Gao, Y., Guieu, C, Ito, A.,
567 Jickells, T.D., Mahowald, M.A., Middag, R., Perron, M.M.G., Sarin, MM., Shelley, R., Turner D.R: Changing
568 atmospheric acidity as a modulator of nutrient deposition and ocean biogeochemistry, *Science Advances*, 2021 (7)
569 eabd8800, 2021
- 570 Barkley, A. E., Prospero, J. M., Mahowald, N., Hamilton, D. S., Popendorf, K. J., Oehlert, A. M., Pourmand, A., Gatineau,
571 A., Panechou-Pulcherie, K., Blackwelder, P., and Gaston, C. J.: African biomass burning is a substantial source of
572 phosphorus deposition to the Amazon, Tropical Atlantic Ocean, and Southern Ocean, *Proceedings of the National
573 Academy of Sciences*, 116, 16216–16221, <https://doi.org/10.1073/pnas.1906091116>, 2019.
- 574 Barraza, F., Lambert, F., Jorquera, H., Villalobos, A. M., and Gallardo, L.: Temporal evolution of main ambient PM2.5
575 sources in Santiago, Chile, from 1998 to 2012, *Atmos Chem Phys*, 17, 10093–10107, <https://doi.org/10.5194/acp-17-10093-2017>, 2017.
- 577 Barrie, L. A., Yi, Y., Leaitch, W. R., Lohmann, U., Kasibhatla, P., Roelofs, G. J., Wilson, J., McGovern, F., Benkovitz, C.,
578 Mélières, M. A., Law, K., Prospero, J., Kritz, M., Bergmann, D., Bridgeman, C., Chin, M., Christensen, J., Easter,
579 R., Feichter, J., Land, C., Jeuken, A., Kjellström, E., Koch, D., and Rasch, P.: A comparison of large-scale
580 atmospheric sulphate aerosol models (COSAM): Overview and highlights, *Tellus B Chem Phys Meteorol*, 53, 615–
581 645, <https://doi.org/10.3402/tellusb.v53i5.16642>, 2001.
- 582 Bauer, S. E., Koch, D., Unger, N., Metzger, S. M., Shindell, D. T., and Streets, D. G.: Nitrate aerosols today and in 2030: a
583 global simulation including aerosols and tropospheric ozone, *Atmos. Chem. Phys.*, 7, 5043–5059,
584 <https://doi.org/10.5194/acp-7-5043-2007>, 2007.
- 585 Bauer, S. E., Tsigaridis, K., and Miller, R.: Significant atmospheric aerosol pollution caused by world food cultivation,
586 *Geophys. Res. Lett.*, 43, 5394–5400, doi:10.1002/2016GL068354, 2016.
- 587 Bauer, S.E., Tsigaridis, K., Faluvegi, G., Nazarenko, L., Miller, R.L., Kelley, M., and Schmidt, G.: The turning point of the
588 aerosol era. *J. Adv. Model. Earth Syst.*, 14, no. 12, e2022MS003070, doi:10.1029/2022MS003070, 2022.
- 589 Bellouin, N., Quaas, J., Gryspenert, E., Kinne, S., Stier, P., Watson-Parris, D., Boucher, O., Carslaw, K. S., Christensen, M.,
590 Daniau, A. L., Dufresne, J. L., Feingold, G., Fiedler, S., Forster, P., Gettelman, A., Haywood, J. M., Lohmann, U.,
591 Malavelle, F., Mauritzen, T., McCoy, D. T., Myhre, G., Mülmenstädt, J., Neubauer, D., Possner, A., Rugenstein,
592 M., Sato, Y., Schulz, M., Schwartz, S. E., Sourdeval, O., Storelvmo, T., Toll, V., Winker, D., and Stevens, B.:
593 Bounding Global Aerosol Radiative Forcing of Climate Change, <https://doi.org/10.1029/2019RG000660>, 1 March
594 2020.



- 595 Bergametti, G., Gomes, L., Doude-Gaussens, G., Rognon, P., and Le Coustumer, M. N: African dust observed over the
596 Canary Islands: source-regions identification and the transport pattern for some summer situations, *J Geophys Res*,
597 94, 14855–14864, 1989.
- 598 Bond, T., Doherty, S. J., Fahey, D., Forster, P., Bernsten, T., DeAngelo, B., Flanner, M., Ghan, S., Karcher, B., Koch, D.,
599 Kinne, S., Kondo, Y., Quinn, P. K., Sarofim, M., Schultz, M., Venkataraman, C., Zhang, H., Zhang, S., Bellouin,
600 N., Guttikunda, S., Hopke, P., Jacobson, M., Kaiser, J. W., Klimont, Z., Lohman, U., Schwartz, J., Shindell, D.,
601 Storelvmo, T., Warren, S., and Zender, C.: Bounding the role of black carbon in the climate system: A scientific
602 assessment, *J Geophys Res*, D118, 5380–5552; doi:10.1002/jgrd_50171, 2013.
- 603 Bond, T. C., Streets, D. G., Yarber, K. F., Nelson, S. M., Woo, J.-H., and Klimont, Z.: A technology-based global inventory
604 of black and organic carbon emissions from combustion, *J Geophys Res*, 109, doi:10.1029/2003JD003697, 2004.
- 605 Bouet, C., Labiad, M. T., Rajot, J. L., Bergametti, G., Marticorena, B., des Tureaux, T. H., Ltifi, M., Sekrafi, S., and Féron,
606 A.: Impact of desert dust on air quality: What is the meaningfulness of daily PM standards in regions close to the
607 sources? The example of Southern Tunisia, *Atmosphere (Basel)*, 10, <https://doi.org/10.3390/atmos10080452>, 2019.
- 608 Bouet, C., Yoboué, V., Marticorena, B., Rajot, J. L., Féron, A., Gaimoz, C., Maisonneuve, F., Siour, G., Valorso, R., Ki, A.
609 F., Konaté, I., and Ouattara, A.: PM10 concentration, Lamto, Côte d'Ivoire, Aeris, 2021.
- 610 Bozlaker, A., Buzcu-Güven, B., Fraser, M. P., and Chellam, S.: Insights into PM10 sources in Houston, Texas: Role of
611 petroleum refineries in enriching lanthanoid metals during episodic emission events, *Atmos Environ*, 69, 109–117,
612 <https://doi.org/10.1016/j.atmosenv.2012.11.068>, 2013.
- 613 Brahney, J., Mahowald, N., Ward, D. S., Ballantyne, A. P., and Neff, J. C.: Is atmospheric phosphorus pollution altering
614 global alpine Lake stoichiometry?, *Global Biogeochem Cycles*, 29, 1369–1383,
615 <https://doi.org/10.1002/2015GB005137>, 2015.
- 616 Brodsky, H., Calderon, R., Hamilton, D. S., Li, L., Miles, A. D., Pavlick, R. P., Gold, K. M., Crandall, S. G., and Mahowald,
617 N. M.: Assessing long-distance atmospheric transport of soilborne plant pathogens, *Environmental Research
Letters*, <https://doi.org/10.1088/1748-9326/acf50c>, 2023.
- 619 Bullard, J., Baddock, M., McTainsh, G., and Leys, J.: Sub-basin scale dust source geomorphology detected using MODIS,
620 *Geophys Res Lett*, 35, <https://doi.org/10.1029/2008GL033928>, 2008.
- 621 Burnett, R., Chen, H., Szyszkowicz, M., Fann, N., Hubbell, B., Pope, C. A., Apte, J. S., Brauer, M., Cohen, A., Weichenthal,
622 S., Coggins, J., Di, Q., Brunekreef, B., Frostad, J., Lim, S. S., Kan, H., Walker, K. D., Thurston, G. D., Hayes, R.
623 B., Lim, C. C., Turner, M. C., Jerrett, M., Krewski, D., Gapstur, S. M., Diver, W. R., Ostro, B., Goldberg, D.,
624 Crouse, D. L., Martin, R. v., Peters, P., Pinault, L., Tjepkema, M., van Donkelaar, A., Villeneuve, P. J., Miller, A.
625 B., Yin, P., Zhou, M., Wang, L., Janssen, N. A. H., Marra, M., Atkinson, R. W., Tsang, H., Thach, T. Q., Cannon, J.
626 B., Allen, R. T., Hart, J. E., Laden, F., Cesaroni, G., Forastiere, F., Weinmayr, G., Jaensch, A., Nagel, G., Concin,
627 H., and Spadaro, J. v.: Global estimates of mortality associated with longterm exposure to outdoor fine particulate
628 matter, *Proc Natl Acad Sci U S A*, 115, 9592–9597, <https://doi.org/10.1073/pnas.1803222115>, 2018.



- 629 Burgos, M. A., E. Andrews, G. Titos, A. Benedetti, H. Bian, V. Buchard, G. Curci, Z. Kipling, A. Kirkevåg, H. Kokkola, A.
630 Laakso, J. Letertre-Danczak, M. T. Lund, H. Matsui, G. Myhre, C. Randles, M. Schulz, T. van Noije, K. Zhang, L.
631 Alados-Arboledas, U. Baltensperger, A. Jefferson, J. Sherman, J. Sun, E. Weingartner, and P. Zieger (2020), A
632 global model-measurement evaluation of particle light scattering coefficients at elevated relative humidity,
633 Atmospheric Chemistry and Physics, 20, 10231–10258, doi:10.5194/acp-20-10231-2020
634 Burrows, S. M., Elbert, W., Lawrence, M. G., and Poschl, U.: Bacteria in the global atmosphere--Part 1:Review and synthesis of literature for
635 different ecosystems, Atmos Chem Phys, 9, 9263–9280, 2009.
- 636 Burrows, S. M., Ogunro, O., Frossard, A. A., Russell, L. M., Rasch, P. J., and Elliott, S. M.: A physically based framework
637 for modeling the organic fractionation of sea spray aerosol from bubble film Langmuir equilibria, Atmos Chem
638 Phys, 14, 13601–13629, <https://doi.org/10.5194/acp-14-13601-2014>, 2014.
- 639 Caldwell, P. M., Mametjanov, A., Tang, Q., van Roekel, L. P., Golaz, J. C., Lin, W., Bader, D. C., Keen, N. D., Feng, Y.,
640 Jacob, R., Maltrud, M. E., Roberts, A. F., Taylor, M. A., Veneziani, M., Wang, H., Wolfe, J. D., Balaguru, K.,
641 Cameron-Smith, P., Dong, L., Klein, S. A., Leung, L. R., Li, H. Y., Li, Q., Liu, X., Neale, R. B., Pinheiro, M., Qian,
642 Y., Ullrich, P. A., Xie, S., Yang, Y., Zhang, Y., Zhang, K., and Zhou, T.: The DOE E3SM Coupled Model Version
643 1: Description and Results at High Resolution, J Adv Model Earth Syst, <https://doi.org/10.1029/2019MS001870>,
644 2019.
- 645 Chatziparaschos, M., Daskalakis, N., Myriokefalitakis, S., Kalivitis, N., Nenes, A., Gonçalves Ageitos, M., Costa-Surós, M.,
646 Pérez García-Pando, C., Zanoli, M., Vrekoussis, M., and Kanakidou, M.: Role of K-feldspar and quartz in global
647 ice nucleation by mineral dust in mixed-phase clouds, Atmos. Chem. Phys., 23, 1785–1801,
648 <https://doi.org/10.5194/acp-23-1785-2023>, 2023.
- 649 Chen, Y., Street, J., and Paytan, A.: Comparison between pure-water- and seawater-soluble nutrient concentrations of
650 aerosol particles from the {Gulf} of {Aqaba}, Mar Chem, 101, 141–152,
651 <https://doi.org/10.1016/j.marchem.2006.02.002>, 2006.
- 652 Chuang, P., Duvall, R., Shafer, M., and Schauer, J.: The origin of water soluble particulate iron in the Asian atmospheric
653 outflow, Geophys Res Lett, 32, doi:10.1029/2004GL021946, 2005.
- 654 Cipoli, Y. A., Alves, C., Rapuano, M., Evtyugina, M., Rienda, I. C., Kováts, N., Vicente, A., Giardi, F., Furst, L., Nunes, T.,
655 and Feliciano, M.: Nighttime–daytime PM10 source apportionment and toxicity in a remoteness inland city of the
656 Iberian Peninsula, Atmos Environ, 303, <https://doi.org/10.1016/j.atmosenv.2023.119771>, 2023.
- 657 Cohen, D., Garton, D., Stelcer, E., Hawas, O., Wang, T., Pon, S., Kim, J., Choi, B., Oh, S., Shin, H.-J., Ko, M., and
658 Uematsu, M.: Multielemental analysis and characterization of fine aerosols at several key ACE-Asia sites, 109,
659 doi:10.1029/2003JD003569, 2004.
- 660 Collaud Coen, M., Andrews, E., Lastuey, A., Petkov Arsov, T., Backman, J., Brem, B. T., Bukowiecki, N., Courret, C.,
661 Eleftheriadis, K., Flentje, H., Fiebig, M., Gysel-Beer, M., Hand, J. L., Hoffer, A., Hooda, R., Hueglin, C., Joubert,
662 W., Keywood, M., Eun Kim, J., Kim, S. W., Labuschagne, C., Lin, N. H., Lin, Y., Lund Myhre, C., Luoma, K.,



- 663 Lyamani, H., Marinoni, A., Mayol-Bracero, O. L., Mihalopoulos, N., Pandolfi, M., Prats, N., Prenni, A. J., Putaud,
664 J. P., Ries, L., Reisen, F., Sellegrí, K., Sharma, S., Sheridan, P., Patrick Sherman, J., Sun, J., Titos, G., Torres, E.,
665 Tuch, T., Weller, R., Wiedensohler, A., Zieger, P., and Laj, P.: Multidecadal trend analysis of in situ aerosol
666 radiative properties around the world, *Atmos Chem Phys*, 20, 8867–8908, <https://doi.org/10.5194/acp-20-8867-2020>, 2020.
- 667 Computational and Information Systems Laboratory: Cheyenne: HPE/SGI ICE XA System (NCAR Community
668 Computing), <https://doi.org/10.5065/D6RX99HX>, 2019.
- 669 da Silva, L. I. D., de Souza Sarkis, J. E., Zotin, F. M. Z., Carneiro, M. C., Neto, A. A., da Silva, A. dos S. A. G., Cardoso, M.
670 J. B., and Monteiro, M. I. C.: Traffic and catalytic converter - Related atmospheric contamination in the
671 metropolitan region of the city of Rio de Janeiro, Brazil, *Chemosphere*, 71, 677–684,
672 <https://doi.org/10.1016/j.chemosphere.2007.10.057>, 2008.
- 673 Dentener, F. J., Carmichael, G. R., Zhang, Y., Lelieveld, J., and Crutzen, P. J.: Role of mineral aerosol as a reactive surface
674 in the global troposphere, *J Geophys Res*, 101, 22,822-869,889, 1996.
- 675 Dentener, F., Kinne, S., Bond, T., Boucher, O., Cofala, J., Generoso, S., Ginoux, P., Gong, S., Hoelzemann, J. J., Ito, A.,
676 Marelli, L., Penner, J., Putaud, J.-P., Textor, C., Schulz, M., van der Werf, G. R., and Wilson, J.: Emissions of
677 primary aerosol and precursor gases in the years 2000 and 1750: prescribed data-sets for AeroCom, *Atmos Chem
678 Phys*, 6, 4321–4344, 2006.
- 679 Despres, V., Huffman, J., Burrows, S. M., Hoose, C., Safatov, A., Buryak, G., Frohlich-Nowoisky, J., Elbert, W., Andreae,
680 M., Polsch, U., and Jaenicke, R.: Primary biological aerosol particles in the atmosphere: a review, *Tellus B*, 64,
681 doi:10.3402/tellusb.v64i0.15598, 2012.
- 682 Dongarrà, G., Manno, E., Varrica, D., and Vultaggio, M.: Mass levels, crustal component and trace elements in PM10 in
683 Palermo, Italy, *Atmos Environ*, 41, 7977–7986, <https://doi.org/10.1016/j.atmosenv.2007.09.015>, 2007.
- 684 Dongarrà, G., Manno, E., Varrica, D., Lombardo, M., and Vultaggio, M.: Study on ambient concentrations of PM10, PM10-
685 2.5, PM2.5 and gaseous pollutants. Trace elements and chemical speciation of atmospheric particulates, *Atmos
686 Environ*, 44, 5244–5257, <https://doi.org/10.1016/j.atmosenv.2010.08.041>, 2010.
- 687 Dubovik, O., Holben, B., Eck, T. F., Smirnov, A., et al.: Variability of absorption and optical properties of key aerosol types
688 observed in worldwide locations, *Journal of Atmospheric Science*, 590–608, 2002.
- 689 Fanourgakis, G. S., Kanakidou, M., Nenes, A., Bauer, S. E., Bergman, T., Carslaw, K. S., Grini, A., Hamilton, D. S.,
690 Johnson, J. S., Karydis, V. A., Kirkevåg, A., Kodros, J. K., Lohmann, U., Luo, G., Makkonen, R., Matsui, H.,
691 Neubauer, D., Pierce, J. R., Schmale, J., Stier, P., Tsagaridis, K., Van Noije, T., Wang, H., Watson-Parris, D.,
692 Westervelt, D. M., Yang, Y., Yoshioka, M., Daskalakis, N., Decesari, S., Gysel-Beer, M., Kalivitis, N., Liu, X.,
693 Mahowald, N. M., Myriokefalitakis, S., Schrödner, R., Sfakianaki, M., Tsimpidi, A. P., Wu, M., and Yu, F.:
694 Evaluation of global simulations of aerosol particle and cloud condensation nuclei number, with implications for
695 cloud droplet formation, *Atmos Chem Phys*, 19, 8591–8617, <https://doi.org/10.5194/acp-19-8591-2019>, 2019.



- 697 Formenti, P., Elbert, W., Maenhaut, W., Haywood, J., and Andreae, M. O.: Chemical composition of mineral dust aerosol
698 during the Saharan Dust Experiment (SHADE) airborne campaign in the Cape Verde region, September 2000, *J.
699 Geophys. Res.*, 108, 8576, doi:10.1029/2002JD002648, 2003.
- 700 Furu, E., Katona-Szabo, I., Angyal, A., Szoboszlai, Z., Török, Z., and Kertész, Z.: The effect of the tramway track construction
701 on the aerosol pollution in Debrecen, Hungary, in: Nuclear Instruments and Methods in Physics Research, Section B:
702 Beam Interactions with Materials and Atoms, 124–130, <https://doi.org/10.1016/j.nimb.2015.08.014>, 2015.
- 703 Furu, E., Angyal, A., Szoboszlai, Z., Papp, E., Török, Z., and Kertész, Z.: Characterization of Aerosol Pollution in Two
704 Hungarian Cities in Winter 2009–2010, *Atmosphere* (Basel), 13, <https://doi.org/10.3390/atmos13040554>, 2022.
- 705 Fuzzi, S., Decesari, S., Facchini, M., Cavalli, F., Emblico, L., Mircea, M., Andreae, M., Trebs, I., Hoffer, A., Guyon, P.,
706 Artaxo, P., Rizzo, L., Lara, L., Pauliquevis, T., Maenhaut, W., et al.: Overview of the inorganic and organic
707 composition of size-segregated aerosol in Rondonia, Brazil from the biomass-burning period to the onset of the wet
708 season., *J Geophys Res*, 112, doi:10.1029/2005JD006741, 2007.
- 709 Gantt, B., Meskhidze, N., Facchini, M. C., Rinaldi, M., Ceburnis, D., and O'Dowd, C. D.: Wind speed dependent size-
710 resolved parameterization for the organic mass fraction of sea spray aerosol, *Atmos Chem Phys*, 11, 8777–8790,
711 <https://doi.org/10.5194/acp-11-8777-2011>, 2011.
- 712 García, M. I., Rodríguez, S., and Alastuey, A.: Impact of North America on the aerosol composition in the North Atlantic
713 free troposphere, *Atmos Chem Phys*, 17, 7387–7404, <https://doi.org/10.5194/acp-17-7387-2017>, 2017.
- 714 Gelaro, R., McCarty, W., Suárez, M. J., Todling, R., Molod, A., Takacs, L., Randles, C. A., Darmenov, A., Bosilovich, M.
715 G., and Reichle, R.: The modern-era retrospective analysis for research and applications, version 2 (MERRA-2), *J
716 Clim*, 30, 5419–5454, 2017.
- 717 Gianini, M. F. D., Gehrig, R., Fischer, A., Ulrich, A., Wichser, A., and Hueglin, C.: Chemical composition of PM10 in
718 Switzerland: An analysis for 2008/2009 and changes since 1998/1999, *Atmos Environ*, 54, 97–106,
719 <https://doi.org/10.1016/j.atmosenv.2012.02.037>, 2012a.
- 720 Gianini, M. F. D., Fischer, A., Gehrig, R., Ulrich, A., Wichser, A., Piot, C., Besombes, J. L., and Hueglin, C.: Comparative
721 source apportionment of PM10 in Switzerland for 2008/2009 and 1998/1999 by Positive Matrix Factorisation,
722 *Atmos Environ*, 54, 149–158, <https://doi.org/10.1016/j.atmosenv.2012.02.036>, 2012b.
- 723 Gidden, M. J., Riahi, K., Smith, S. J., Fujimori, S., Luderer, G., Kriegler, E., Van Vuuren, D. P., Van Den Berg, M., Feng,
724 L., Klein, D., Calvin, K., Doelman, J. C., Frank, S., Fricko, O., Harmsen, M., Hasegawa, T., Havlik, P., Hilaire, J.,
725 Hoesly, R., Horing, J., Popp, A., Stehfest, E., and Takahashi, K.: Global emissions pathways under different
726 socioeconomic scenarios for use in CMIP6: A dataset of harmonized emissions trajectories through the end of the
727 century, *Geosci Model Dev*, 12, 1443–1475, <https://doi.org/10.5194/gmd-12-1443-2019>, 2019.
- 728 Ginoux, P., Chin, M., Tegen, I., Prospero, J. M., Holben, B. N., Dubovik, O., and Lin, S.-J.: Sources and distribution of dust
729 aerosol particles with the GOCART model, *J Geophys Res*, 106, 20255–20273, 2001.



- 730 Ginoux, P., Prospero, J., Gill, T. E., Hsu, N. C., and Zhao, M.: Global scale attribution of anthropogenic and natural dust
731 sources and their emission rates based on MODIS deep blue aerosol products, *Reviews of Geophysics*, 50,
732 DOI:10.1029/2012RG000388, 2012.
- 733 Gliß, J., Mortier, A., Schulz, M., Andrews, E., Balkanski, Y., Bauer, S. E., Benedictow, A. M. K., Bian, H., Checa-Garcia,
734 R., Chin, M., Ginoux, P., Griesfeller, J. J., Heckel, A., Kipling, Z., Kirkevåg, A., Kokkola, H., Laj, P., Le Sager, P.,
735 Lund, T. M., Lund Myhre, C., Matsui, H., Myhre, G., Neubauer, D., Van Noije, T., North, P., Olivié, D. J. L.,
736 Rémy, S., Sogacheva, L., Takemura, T., Tsigaridis, K., and Tsyro, S. G.: AeroCom phase III multi-model
737 evaluation of the aerosol life cycle and optical properties using ground- And space-based remote sensing as well as
738 surface in situ observations, *Atmos Chem Phys*, 21, 87–128, <https://doi.org/10.5194/acp-21-87-2021>, 2021.
- 739 Golaz, J. C., Caldwell, P. M., van Roekel, L. P., Petersen, M. R., Tang, Q., Wolfe, J. D., Abeshu, G., Anantharaj, V., Asay-
740 Davis, X. S., Bader, D. C., Baldwin, S. A., Bisht, G., Bogenschutz, P. A., Branstetter, M., Brunke, M. A., Brus, S.
741 R., Burrows, S. M., Cameron-Smith, P. J., Donahue, A. S., Deakin, M., Easter, R. C., Evans, K. J., Feng, Y.,
742 Flanner, M., Foucar, J. G., Fyke, J. G., Griffin, B. M., Hannay, C., Harrop, B. E., Hoffman, M. J., Hunke, E. C.,
743 Jacob, R. L., Jacobsen, D. W., Jeffery, N., Jones, P. W., Keen, N. D., Klein, S. A., Larson, V. E., Leung, L. R., Li,
744 H. Y., Lin, W., Lipscomb, W. H., Ma, P. L., Mahajan, S., Maltrud, M. E., Mametjanov, A., McClean, J. L., McCoy,
745 R. B., Neale, R. B., Price, S. F., Qian, Y., Rasch, P. J., Reeves Eyre, J. E. J., Riley, W. J., Ringler, T. D., Roberts, A.
746 F., Roesler, E. L., Salinger, A. G., Shaheen, Z., Shi, X., Singh, B., Tang, J., Taylor, M. A., Thornton, P. E., Turner,
747 A. K., Veneziani, M., Wan, H., Wang, H., Wang, S., Williams, D. N., Wolfram, P. J., Worley, P. H., Xie, S., Yang,
748 Y., Yoon, J. H., Zelinka, M. D., Zender, C. S., Zeng, X., Zhang, C., Zhang, K., Zhang, Y., Zheng, X., Zhou, T., and
749 Zhu, Q.: The DOE E3SM Coupled Model Version 1: Overview and Evaluation at Standard Resolution, *J Adv
750 Model Earth Syst*, 11, 2089–2129, <https://doi.org/10.1029/2018MS001603>, 2019.
- 751 Gonçalves Ageitos, M., V. Obiso, R.L. Miller, O. Jorba, M. Klose, M. Dawson, Y. Balkanski, J. Perlitz, S. Basart, E. Di
752 Tomaso, J. Escribano, F. Macchia, G. Montané, N. Mahowald, R.O. Green, D.R. Thompson, and C. Pérez García-
753 Pando, 2023: Modeling dust mineralogical composition: sensitivity to soil mineralogy atlases and their expected
754 climate impacts. *Atmos. Chem. Phys.*, 23, no. 15, 8623-8657, doi:10.5194/acp-23-8623-2023.
- 755
- 756 Gong, S. L., Barrie, L. A., Prospero, J. M., Savoie, D. L., Ayers, G. P., Blanchet, J.-P., and Spacek, L.: Modeling sea-salt
757 aerosol particles in the atmosphere 2. Atmospheric concentrations and fluxes, *J Geophys Res*, 102, 3819–3830,
758 1997.
- 759 Gong, S. L., Zhang, X. Y., Zhao, T. L., McKendry, I. G., Jaffe, D. A., and Lu, N. M.: Characterization of soil dust aerosol in
760 China and its transport and distribution during 2001 ACE-Asia: 2. Model simulation and validation, *J Geophys Res*,
761 108, 4262, 2003.
- 762 Graham, B., Guyon, P., Maenhaut, W., Taylor, P. E., Ebert, M., Matthias-Maser, S., Mayol-Bracero, O. L., Godoi, R. H. M.,
763 Artaxo, P., Meixner, F. X., Moura, M. A. L., Rocha, C. H. E., Van Grieken, R., Globsky, M. M., Flagan, R. C., and



- 764 Andreae, M. O.: Composition and diurnal variability of the natural Amazonian aerosol, *J Geophys Res*, 108, 4765,
765 doi:10.1029/2003JD004049, 2003.
- 766 Gulev, S. K., Thorne, P. W., Ahn, J., Dentener, F. J., Domingues, C. M., Gerland, S., Gong, D., Kaufman, D. S., Nnamchi,
767 H. C., Quaas, J., Rivera, J. A., Sathyendranath, S., Smith, S. L., Trewin, B., von Schuckmann, K., and Vose, R. ,S.:
768 Chapter 2: Changing State of the Climate System., in: *Climate Change 2021: The Physical Science Basis*.
769 Contribution of Working Group I to the Sixth Assessment Report of the Intergovernmental Panel on Climate
770 Change, edited by: Masson-Delmotte, V. , Zhai, P., Pirani, A., Connors, S. L., Péan, C., Berger, S., Caud, N., Chen,
771 Y., Goldfarb, L., Gomis, M. I., Huang, M., Leitzell, K., Lonnoy, E., Matthews, J. B. R., Maycock, T. K.,
772 Waterfield, T., Yelekçi, O., Yu, R., and Zhou, B. Cambridge University Press, Cambridge, United Kingdom and
773 New York, NY, USA, 287–422, <https://doi.org/10.1017/9781009157896.004>, 2021.
- 774 Hand, J. L., Gill, T. E., and Schichtel, B. A.: Spatial and seasonal variability in fine mineral dust and coarse aerosol mass at
775 remote sites across the United States, *J Geophys Res*, 122, 3080–3097, <https://doi.org/10.1002/2016JD026290>,
776 2017.
- 777 Hand, J. L., Gill, T. E., and Schichtel, B. A.: Urban and rural coarse aerosol mass across the United States: Spatial and
778 seasonal variability and long-term trends, *Atmos Environ*, 218, 117025,
779 <https://doi.org/10.1016/j.atmosenv.2019.117025>, 2019.
- 780 Hansen, J. and Nazarenko, L.: Soot climate forcing via snow and ice albedos, *PNAS*, 101, 423–428,
781 doi:10.1073/pnas.ss37157100, 2004.
- 782 Heald, C. and Spracklen, D.: Atmospheric budget of primary biological aerosol particles from fungal sources, *Geophys Res
783 Lett*, 36, doi:10.1029/2009GL037493, 2009.
- 784 Heald, C., Ridley, D., Kreidenweis, S., and Drury, E.: Satellite observations cap the atmospheric organic aerosol budget,
785 *Geophys Res Lett*, 37, L24808; doi:10.1029/2010GL045095, 2010.
- 786 Heimburger, A., Losno, R., Triquet, S., Dulac, F., and Mahowald, N.: Direct measurement of atmospheric iron, cobalt and
787 aluminum-derived dust deposition at Kerguelen Islands, *Global Biogeochem Cycles*, 26,
788 doi:10.1029/2012GB004301, <https://doi.org/10.1029/2012GB004301>, 2012.
- 789 Herut, B. and Krom, M.: Atmospheric input of nutrients and dust to the SE Mediterranean, in: *The Impact of Desert Dust
790 Across the Mediterranean* , edited by: Guerzoni, S. and Chester, R., 349–360, 1996.
- 791 Herut, B., Nimmo, M., Medway, A., Chester, R., and Krom, M.D.: Dry atmospheric inputs of trace metals at the
792 Mediterranean coast of Israel (SE Mediterranean): sources and fluxes. *Atmos. Environ.*, 35, 803-813, 2001.
- 793 Hinds, W. C., *Aerosol Technology, Properties, Behavior and Measurement of Airborne Particles*, John Wiley, New York,
794 1999.
- 795 .Hsu, C. Y., Chiang, H. C., Lin, S. L., Chen, M. J., Lin, T. Y., and Chen, Y. C.: Elemental characterization and source
796 apportionment of PM10 and PM2.5 in the western coastal area of central Taiwan, *Science of the Total
797 Environment*, 541, 1139–1150, <https://doi.org/10.1016/j.scitotenv.2015.09.122>, 2016.



- 798 Huang, Y., Adebiyi, A. A., Formenti, P., and Kok, J. F.: Linking the Different Diameter Types of Aspherical Desert Dust
799 Indicates That Models Underestimate Coarse Dust Emission, *Geophys Res Lett*, 48,
800 <https://doi.org/10.1029/2020GL092054>, 2021.
- 801 Hueglin, C., Gehrig, R., Baltensperger, U., Gysel, M., Monn, C., and Vonmont, H.: Chemical characterisation of PM2.5,
802 PM10 and coarse particles at urban, near-city and rural sites in Switzerland, *Atmos Environ*, 39, 637–651,
803 <https://doi.org/10.1016/j.atmosenv.2004.10.027>, 2005.
- 804 Huneeus, N., Schulz, M., Balkanski, Y., Griesfeller, J., Prospero, J., Kinne, S., Bauer, S., Boucher, O., Chin, M., Dentener,
805 F., Diehl, T., Easter, R., Fillmore, D., Ghan, S., Ginoux, P., Grini, A., Horowitz, L., Koch, D., Krol, M. C.,
806 Landing, W., Liu, X., Mahowald, N., Miller, R., Morcrette, J.-J., Myhre, G., Penner, J., Perlitz, J., Stier, P.,
807 Takemura, T., and Zender, C. S.: Global dust model intercomparison in AeroCom phase i, *Atmos Chem Phys*, 11,
808 <https://doi.org/10.5194/acp-11-7781-2011>, 2011.
- 809 Hurrell, J. W., Holland, M. M., Gent, P. R., Ghan, S., Kay, J. E., Kushner, P. J., Lamarque, J.-F., Large, W. G., Lawrence,
810 D., Lindsay, K., Lipscomb, W. H., Long, M. C., Mahowald, N., Marsh, D. R., Neale, R. B., Rasch, P., Vavrus, S.,
811 Vertenstein, M., Bader, D., Collins, W. D., Hack, J. J., Kiehl, J., and Marshall, S.: The community earth system
812 model: A framework for collaborative research, *Bull Am Meteorol Soc*, 94, <https://doi.org/10.1175/BAMS-D-12-00121.1>, 2013.
- 813 IPCC: Summary for Policymakers, in: Climate Change 2021: The Physical Science Basis. Contribution of Working Group I
814 to the Sixth Assessment Report of the Intergovernmental Panel on Climate Change, edited by: Masson-Delmotte, V.
815 , P., Zhai, A., Pirani, S.L., Connors, C., Péan, S., Berger, N., Caud, Y., Chen, L., Goldfarb, M. I., Gomis, M.,
816 Huang, K., Leitzell, E., Lonnoy, J. B. R., Matthews, T. B. R., Maycock, T. K., Waterfield, T., Yelekçi, O., Yu, R.,
817 and Zhou B., Cambridge University Press, Cambridge, UK, 3–32, <https://doi.org/10.1017/9781009157896.001>,
818 2021.
- 819 Jaenicke, R.: Abundance of cellular material and proteins in the atmosphere, *Science* (1979), 308, 73,
820 <https://doi.org/10.1126/science.1106335>, 2005.
- 821 Janssen, R., Heald, C., Steiner, A., Perring, A., Huffman, J. A., Robinson, E., Twohy, C., and Ziemba, L.: Drivers of the
822 fungal spore bioaerosol budget: observational analysis and global modelling, *Atmos Chem Phys*, 1–36,
823 <https://doi.org/10.5194/acp-2020-569>, 2020.
- 824 Jensen, J. B. and Lee, S.: Giant sea-salt aerosols and warm rain formation in marine stratocumulus, *J Atmos Sci*, 65, 3678–
825 3694, <https://doi.org/10.1175/2008JAS2617.1>, 2008.
- 826 Kahn, R. A., Gaitley, B., Martonchik, J., Diner, D. J., Crean, K., and Holben, B.: MISR global aerosol optical depth
827 validation based on two years of coincident AERONET observations, *J Geophys Res*, 110,
828 doi:10.1029/2004JD004706, 2005.
- 829 Kalivitis, N., E. Gerasopoulos, M. Vrekoussis, G. Kouvarakis, N. Kubilay, N. Hatzianastassiou, I. Vardavas, and N.
830 Mihalopoulos (2007), Dust transport over the eastern Mediterranean derived from Total Ozone Mapping



- 832 Spectrometer, Aerosol Robotic Network, and surface measurements, *J. Geophys. Res.*, 112, D03202,
833 doi:10.1029/2006JD007510.
- 834 Kaly, F., Marticorena, B., Chatenet, B., Rajot, J. L., Janicot, S., Niang, A., Yahia, H., Thiria, S., Maman, A., Zakou, A.,
835 Coulibaly, B. S., Coulibaly, M., Koné, I., Traoré, S., Diallo, A., and Ndiaye, T.: Variability of mineral dust
836 concentrations over West Africa monitored by the Sahelian Dust Transect, *Atmos Res.*, 164–165, 226–241,
837 https://doi.org/10.1016/j.atmosres.2015.05.011, 2015
- 838 Kanakidou, M., Seinfeld, J., Pandis, S., Barnes, I., Dentener, F., Facchini, M., et al.: Organic aerosol and global climate
839 modeling: a review, *Atmos Chem Phys*, 5, 1053–1123, 2005.
- 840 Kanakidou M., Myriokefalitakis S., Tsagaridis K.: Aerosols in atmospheric chemistry and biogeochemical cycles of
841 nutrients, *Environ. Res. Lett.* 13 063004, 2018. https://doi.org/10.1088/1748-9326/aabcb
- 842 Karydis, V. A., Tsimpidi, A. P., Bacer, S., Pozzer, A., Nenes, A., and Lelieveld, J.: Global impact of mineral dust on cloud
843 droplet number concentration, *Atmos. Chem. Phys.*, 17, 5601–5621, https://doi.org/10.5194/acp-17-5601-2017,
844 2017.
- 845 Klimont, Z., Kupiainen, K., Heyes, C., Purohit, P., Cofala, J., Rafaj, P., Borken-Kleefeld, J., and Schöpp, W.: Global
846 anthropogenic emissions of particulate matter including black carbon, *Atmos Chem Phys*, 17, 8681–8723,
847 https://doi.org/10.5194/acp-17-8681-2017, 2017.
- 848 Koch, D., Schulz, M., Kinne, S., McNaughton, C., et al.: Evaluation of black carbon estimations in global aerosol models,
849 *Atmos Chem Phys*, 9, 9001–9026, 2009.
- 850 Kok, J. F., Mahowald, N. M., Fratini, G., Gillies, J. A., Ishizuka, M., Leys, J. F., Mikami, M., Park, M.-S., Park, S.-U., van
851 Pelt, R. S., and Zobeck, T. M.: An improved dust emission model - Part 1: Model description and comparison
852 against measurements, *Atmos Chem Phys*, 14, https://doi.org/10.5194/acp-14-13023-2014, 2014a.
- 853 Kok, J. F., Albani, S., Mahowald, N. M., and Ward, D. S.: An improved dust emission model - Part 2: Evaluation in the
854 Community Earth System Model, with implications for the use of dust source functions, *Atmos Chem Phys*, 14,
855 https://doi.org/10.5194/acp-14-13043-2014, 2014b.
- 856 Kok, J. F., Ridley, D. A., Zhou, Q., Miller, R. L., Zhao, C., Heald, C. L., Ward, D. S., Albani, S., and Haustein, K.: Smaller
857 desert dust cooling effect estimated from analysis of dust size and abundance, *Nat Geosci.*, 10, 274–278,
858 https://doi.org/10.1038/ngeo2912, 2017.
- 859 Kok, J. F., Adebiyi, A. A., Albani, S., Balkanski, Y., Checa-Garcia, R., Chin, M., Colarco, P. R., Hamilton, D. S., Huang, Y.,
860 Ito, A., Klose, M., Leung, D. M., Li, L., Mahowald, N. M., Miller, R. L., Obiso, V., Pérez García-Pando, C., Rocha-
861 Lima, A., Wan, J. S., and Whicker, C. A.: Improved representation of the global dust cycle using observational
862 constraints on dust properties and abundance, *Atmos Chem Phys*, 21, 8127–8167, https://doi.org/10.5194/acp-21-
863 8127-2021, 2021.
- 864 Kubilay, N., Nickovic, S., Moulin, C., and Dulac, F.: An illustration of the transport and deposition of mineral dust onto the
865 eastern Mediterranean, *Atmos Environ.*, 34, 1293–1303, 2000.



- 866 Kyllönen, K., Vestenius, M., Anttila, P., Makkonen, U., Aurela, M., Wängberg, I., Nerentorp Mastromonaco, M., and
867 Hakola, H.: Trends and source apportionment of atmospheric heavy metals at a subarctic site during 1996–2018,
868 *Atmos Environ*, 236, <https://doi.org/10.1016/j.atmosenv.2020.117644>, 2020.
- 869 Laing, J. R., Hopke, P. K., Hopke, E. F., Husain, L., Dutkiewicz, V. A., Paatero, J., and Viisanen, Y.: Long-term particle
870 measurements in finnish arctic: Part I - Chemical composition and trace metal solubility, *Atmos Environ*, 88, 275–
871 284, <https://doi.org/10.1016/j.atmosenv.2014.03.002>, 2014a.
- 872 Laing, J. R., Hopke, P. K., Hopke, E. F., Husain, L., Dutkiewicz, V. A., Paatero, J., and Viisanen, Y.: Long-term particle
873 measurements in finnish arctic: Part II - trend analysis and source location identification, *Atmos Environ*, 88, 285–
874 296, <https://doi.org/10.1016/j.atmosenv.2014.01.015>, 2014b.
- 875 Laj, P., Bigi, A., Rose, C., Andrews, E., Lund Myhre, C., Collaud Coen, M., Lin, Y., Wiedensohler, A., Schulz, M., A.
876 Ogren, J., Fiebig, M., Gliß, J., Mortier, A., Pandolfi, M., Petäja, T., Kim, S. W., Aas, W., Putaud, J. P., Mayol-
877 Bracero, O., Keywood, M., Labrador, L., Aalto, P., Ahlberg, E., Alados Arboledas, L., Alastuey, A., Andrade, M.,
878 Artinano, B., Ausmeel, S., Arsov, T., Asmi, E., Backman, J., Baltensperger, U., Bastian, S., Bath, O., Paul Beukes,
879 J., T. Brem, B., Bukowiecki, N., Conil, S., Couret, C., Day, D., Dayantolis, W., Degorska, A., Eleftheriadis, K.,
880 Fetfatzis, P., Favez, O., Flentje, H., I. Gini, M., Gregorić, A., Gysel-Beer, M., Gannet Hallar, A., Hand, J., Hoffer,
881 A., Hueglin, C., K. Hooda, R., Hyvärinen, A., Kalapov, I., Kalivitis, N., Kasper-Giebl, A., Eun Kim, J., Kouvarakis,
882 G., Kranjc, I., Krejci, R., Kulmala, M., Labuschagne, C., Lee, H. J., Lihavainen, H., Lin, N. H., Löschau, G.,
883 Luoma, K., Marinoni, A., Martins Dos Santos, S., Meinhardt, F., Merkel, M., Metzger, J. M., Mihalopoulos, N.,
884 Anh Nguyen, N., Ondracek, J., Pérez, N., Rita Perrone, M., Pichon, J. M., Picard, D., Pichon, J. M., Pont, V., Prats,
885 N., Prenni, A., Reisen, F., Romano, S., Sellegri, K., Sharma, S., Schauer, G., Sheridan, P., Patrick Sherman, J.,
886 Schütze, M., Schwerin, A., Sohmer, R., Sorribas, M., Steinbacher, M., Sun, J., Titos, G., et al.: A global analysis of
887 climate-relevant aerosol properties retrieved from the network of Global Atmosphere Watch (GAW) near-surface
888 observatories, *Atmos Meas Tech*, 13, 4353–4392, <https://doi.org/10.5194/amt-13-4353-2020>, 2020.
- 889 Li, J., Carlson, B. E., Yung, Y. L., Lv, D., Hansen, J., Penner, J. E., Liao, H., Ramaswamy, V., Kahn, R. A., Zhang, P.,
890 Dubovik, O., Ding, A., Lacis, A. A., Zhang, L., and Dong, Y.: Scattering and absorbing aerosols in the climate
891 system, <https://doi.org/10.1038/s43017-022-00296-7>, 1 June 2022a.
- 892 Li, L., Mahowald, N. M., Miller, R. L., Pérez Garcíá-Pando, C., Klose, M., Hamilton, D. S., Gonçalves Ageitos, M., Ginoux,
893 P., Balkanski, Y., Green, R. O., Kalashnikova, O., Kok, J. F., Obiso, V., Paynter, D., and Thompson, D. R.:
894 Quantifying the range of the dust direct radiative effect due to source mineralogy uncertainty, *Atmos Chem Phys*,
895 21, 3973–4005, <https://doi.org/10.5194/acp-21-3973-2021>, 2021.
- 896 Li, L., Mahowald, N. M., Kok, J. F., Liu, X., Wu, M., Leung, D. M., Hamilton, D. S., Emmons, L. K., Huang, Y., Meng, J.,
897 Sexton, N., and Wan, J.: Importance of different parameterization changes for the updated dust cycle modelling in
898 the Community Atmosphere Model (version 6.1), *Geoscientific Model Development Discussion*,
899 <https://doi.org/10.5194/gmd-2022-31>, 2022.



- 900 Lim, S. S., Vos, T., Flaxman, A. D., Danaei, G., Shibuya, K., Adair-Rohani, H., and AlMazroa, M. ; A comparative risk
901 assessment of burden of disease and injury attributable to 67 risk factors and risk factor clusters in 21 regions,
902 1990–2010: A systematic analysis for the Global Burden of Disease Study 2010., Lancet, 380, 2224–2260, 2012.
903 Liu, X., REaster, R. C., Ghan, S. J., Zaveri, R., Rasch, P., Shi, X., Lamarque, J.-F., Gettelman, A., Morrison, H., Vitt, F.,
904 Conley, A., Park, S., Neale, R., Hannay, C., Ekman, A., Hess, P., Mahowald, N., Collins, W., Iacono, M.,
905 Bretherton, C., Flanner, M., and Mitchell, D: Toward a minimal representation of aerosols in climate models:
906 Description and evaluation in the Community Atmosphere Model CAM5, Geoscientific Model Development, 5,
907 709-739, doi:10.5194/gmd-5-709-2012, 2012.
908 Liu, X., Ma, P. L., Wang, H., Tilmes, S., Singh, B., Easter, R. C., Ghan, S. J., and Rasch, P. J.: Description and evaluation of
909 a new four-mode version of the Modal Aerosol Module (MAM4) within version 5.3 of the Community Atmosphere
910 Model, Geosci Model Dev, 9, 505–522, <https://doi.org/10.5194/gmd-9-505-2016>, 2016.
911 Lucarelli, F., Calzolai, G., Chiari, M., Giannoni, M., Mochi, D., Nava, S., and Carraresi, L.: The upgraded external-beam
912 PIXE/PIGE set-up at LABEC for very fast measurements on aerosol samples, Nucl Instrum Methods Phys Res B,
913 318, 55–59, <https://doi.org/10.1016/j.nimb.2013.05.099>, 2014.
914 Lucarelli, F., Barrera, V., Becagli, S., Chiari, M., Giannoni, M., Nava, S., Traversi, R., and Calzolai, G.: Combined use of
915 daily and hourly data sets for the source apportionment of particulate matter near a waste incinerator plant,
916 Environmental Pollution, 247, 802–811, <https://doi.org/10.1016/j.envpol.2018.11.107>, 2019.
917
918 Mackey, K. R. M., Hunter, D., Fischer, E. V., Jiang, Y., Allen, B., Chen, Y., Liston, A., Reuter, J., Schladow, G., and Paytan,
919 A.: Aerosol-nutrient-induced picoplankton growth in Lake Tahoe, J Geophys Res Biogeosci, 118, 1054–1067,
920 <https://doi.org/10.1002/jgrg.20084>, 2013.
921 Maenhaut, W., Cafmeyer, J., Ptasinski, J., Andreae, M. O., Andreae, T. W., Elbert, W., Meixner, F. X., Karnieli, A., and
922 Ichoku, C.: Chemical composition and light scattering of the atmospheric aerosol at a remote site in the Negev
923 desert, Israel, J. Aerosol Sci., 28 (suppl.), 73–74, 1997b.
924 Maenhaut, W. and Cafmeyer, J.: Long-Term Atmospheric Aerosol Study at Urban and Rural Sites in Belgium Using Multi-
925 Elemental Analysis by Particle-Induced X-Ray Emission Spectrometry and Short-Irradiation Instrumental Neutron
926 Activation Analysis, X-Ray Spectrometry, 27, 236–246, [https://doi.org/10.1002/\(SICI\)1097-4539\(199807/08\)27:4<236::AID-XRS292>3.0.CO;2-F](https://doi.org/10.1002/(SICI)1097-4539(199807/08)27:4<236::AID-XRS292>3.0.CO;2-F), 1998.
927
928 Maenhaut, W., Salomonovic, R., Cafmeyer, J., Ichoku, C., Karnieli, A., and Andreae, M. O.: Anthropogenic and natural
929 radiatively active aerosol types at Sede Boker, Israel, J. Aerosol Sci., 27 (suppl., 47–48,
930 [https://doi.org/10.1016/0021-8502\(96\)00096-1](https://doi.org/10.1016/0021-8502(96)00096-1), 1996a.
931 Maenhaut, W., Koppen, G., and Artaxo, P.: Long-term atmospheric aerosol study in Cuiaba', Brazil: Multielemental
932 composition, sources, and impact of biomass burning, in: Biomass Burning and Global Change, vol. 2, Biomass



- 933 Burning in South America, Southeast Asia, and Temperate and Boreal Ecosystems, and the Oil Fires of Kuwait,
934 edited by: Levine, J. S., MIT Press, Cambridge Massachusetts, 637–652, 1996b.
- 935 Maenhaut, W., Salma, I., Cafmeyer, J., Annegard, H., and Andreae, M.: Regional atmospheric aerosol composition and
936 sources in the eastern Transvaal, South Africa and impact of biomass burning, *J Geophys Res*, 101, 23631–23650,
937 1996c.
- 938 Maenhaut, W., Francois, F., Cafmeyer, J., Gilot, C., and Hanssen, J. E.: Long-term aerosol study in southern Norway, and
939 the relationship of aerosol components to source, in: *Proceedings of EUROTAC Symposium '96*, vol. 1, *Clouds,*
940 *Aerosols, Modelling and Photo-oxidants*, edited by: Borrell, P. M., Comput. Mech. Publ., South Hampton, UK),
941 277–280, 1997a.
- 942 Maenhaut, W., Fernandez-Jimenez, M.-T., and Artaxo, P.: Long-term study of atmospheric aerosols in Cuiaba, Brazil:
943 Multielemental composition, sources and source apportionment, *J. Aerosol Sci.*, 30 (suppl., 259–260, 1999.
- 944 Maenhaut, W., Fernandez-Jimenez, M.-T., Vanderzalm, J. L., Hooper, B., Hooper, M. A., and Tapper, N. J.: Aerosol
945 composition at Jabiru, Australia, and impact of biomass burning, *J. Aerosol Sci.*, 31 (suppl., 745–746,
946 [https://doi.org/10.1016/S0021-8502\(00\)90755-9](https://doi.org/10.1016/S0021-8502(00)90755-9), 2000a.
- 947 Maenhaut, W., Fernandez-Jimenez, M.-T., Rajta, I., Dubtsov, S., Meixner, F. X., Andreae, M. O., Torr, S., Hargrove, J. W.,
948 Chimanga, P., and Mlambo, J.: Long-term aerosol composition measurements and source apportionment at
949 Rukomechi, Zimbabwe, *J. Aerosol Sci.*, 31 (suppl., 228–229, [https://doi.org/10.1016/S0021-8502\(00\)90237-4](https://doi.org/10.1016/S0021-8502(00)90237-4),
950 2000b.
- 951 Maenhaut, W., De Ridder, D. J. A., Fernandez-Jimenez, M.-T., Hooper, M. A., Hooper, B., and Nurhayati, M.: Long-term
952 observations of regional aerosol composition at two sites in Indonesia, *Nucl. Instrum. Methods Phys. Res., Sect. B.*,
953 189, 259–265, [https://doi.org/10.1016/S0168- 583X\(01\)01054-0](https://doi.org/10.1016/S0168- 583X(01)01054-0), 2002a.
- 954 Maenhaut, W., Fernandez-Jimenez, M.-T., Rajta, I., and Artaxo, P.: Two-year study of atmospheric aerosol particles in Alta
955 Floresta, Brazil: Multielemental composition and source apportionment, *Nuclear Instruments and Methods in*
956 *Physics Research B*, 189, 243–248, 2002b.
- 957 Maenhaut, W., Raes, N., Chi, X., Cafmeyer, J., Wang, W., and Salma, I.: Chemical composition and mass closure for fine
958 and coarse aerosols at a kerbside in Budapest, Hungary, in spring 2002, *X-Ray Spectrometry*, 34, 290–296,
959 <https://doi.org/10.1002/xrs.820>, 2005.
- 960 Maenhaut, W., Raes, N., Chi, X., Cafmeyer, J., and Wang, W.: Chemical composition and mass closure for PM2.5 and PM
961 10 aerosols at K-puszta, Hungary, in summer 2006, in: *X-Ray Spectrometry*, 193–197,
962 <https://doi.org/10.1002/xrs.1062>, 2008.
- 963 Maenhaut, W., Nava, S., Lucarelli, F., Wang, W., Chi, X., and Kulmala, M.: Chemical composition, impact from biomass
964 burning, and mass closure for PM2.5 and PM10 aerosols at Hyttiälä, Finland, in summer 2007, *X-Ray*
965 *Spectrometry*, 40, 168–171, <https://doi.org/10.1002/xrs.1302>, 2011.
- 966



- 967 Mahowald, N., Li, L., Vira, J., Prank, M., Hamilton, D. S., Matsui, H., Miller, R. L., Lu, L., Akyuz, E. A., Daphne, M., Hess,
968 P., Lihavainen, H., Wiedinmyer, C., Hand, J., Alaimo, M. G., Alves, C., Alastuey, A., Artaxo, P., Barreto, A.,
969 Barraza, F., Becagli, S., Calzolai, G., Chellam, S., Chen, Y., Chuang, P., Cohen, D., Colombi, C., Diapouli, E.
970 Dongarra, G., Eleftheriadis, K., Galy-Lacaux, C., Gaston, C., Gomez, D., Gonzalez Ramos, Y., Hakola, H.,
971 Harrison, R., Heyes, C., Herut, B., Hopke, P., Huglin, C., Kanakidou, M., Kertesz, Z., Klimont, Z., Kyllonen, K.,
972 Lambert, F., Liu, X., Losno, R., Lucarelli, F., Maenhaut, W., Marticorena, B., Martin, R., Mihalopoulos, N.,
973 Morera-Gomez, Y., Paytan, A., Prospero, J., Rodriguez, S., Smichowski, P., Varrica, D., Walsh, B., Weagle, C.,
974 Zhao, X. (2024). Datasets for: AERO-MAP: A data compilation and modelling approach to understand the fine and
975 coarse mode aerosol composition (January 4, 2024 version) [Data set]. Zenodo.
976 <https://doi.org/10.5281/zenodo.10459654>
- 977 Mahowald, N., Artaxo, P., Baker, A., Jickells, T., Okin, G., Randerson, J., and Townsend, A.: Impact of biomass burning
978 emissions and land use change on Amazonian atmospheric cycling and deposition of phosphorus, Global
979 Biogeochem Cycles, 19, GB4030; 10.1029/2005GB002541, 2005.
- 980 Mahowald, N., Lamarque, J.-F., Tie, X., and Wolff, E.: Sea salt aerosol response to climate change: last glacial maximum,
981 pre-industrial, and doubled-carbon dioxide climates, J Geophys Res, 111, D05303; doi:10.1029/2005JD006459,
982 2006.
- 983 Mahowald, N., Jickells, T. D., Baker, A. R., Artaxo, P., Benitez-Nelson, C. R., Bergametti, G., Bond, T. C., Chen, Y.,
984 Cohen, D. D., Herut, B., Kubilay, N., Losno, R., Luo, C., Maenhaut, W., McGee, K. A., Okin, G. S., Siebert, R. L.,
985 and Tsukuda, S.: Global distribution of atmospheric phosphorus sources, concentrations and deposition rates, and
986 anthropogenic impacts, Global Biogeochem Cycles, 22, <https://doi.org/10.1029/2008GB003240>, 2008.
- 987 Mahowald, N., Ward, D. S., Kloster, S., Flanner, M. G., Heald, C. L., Heavens, N. G., Hess, P. G., Lamarque, J.-F., and
988 Chuang, P. Y.: Aerosol Impacts on Climate and Biogeochemistry, Annu Rev Environ Resour, 36, 45–74,
989 <https://doi.org/10.1146/annurev-environ-042009-094507>, 2011.
- 990 Mahowald, N., Albani, S., Kok, J. F., Engelstaeder, S., Scanza, R., Ward, D. S., and Flanner, M. G.: The size distribution of
991 desert dust aerosol particles and its impact on the Earth system, Aeolian Res, 15, 53–71,
992 <https://doi.org/https://doi.org/10.1016/j.aeolia.2013.09.002>, 2014a.
- 993 Mahowald, N., Albani, S., Kok, J. F., Engelstaeder, S., Scanza, R., Ward, D. S., and Flanner, M. G.: The size distribution of
994 desert dust aerosol particles and its impact on the Earth system, Aeolian Res, 15,
995 <https://doi.org/10.1016/j.aeolia.2013.09.002>, 2014b.
- 996 Mahowald, N. M., Engelstaedter, S., Luo, C., Sealy, A., Artaxo, P., Benitez-Nelson, C., Bonnet, S., Chen, Y., Chuang, P. Y.,
997 Cohen, D., Dulac, F., Herut, B., Johansen, A. M., Kubilay, N., Losno, R., Maenhaut, W., Paytan, A., Prospero, J.
998 M., Shank, L. M., and Siebert, R. L.: Atmospheric Iron Deposition: Global Distribution, Variability, and Human
999 Perturbations, Annual Review of Marine Science of Marine Science, 1, 245–278,
1000 <https://doi.org/10.1146/annurev.marine.010908.163727>, 2009.



- 1001 Mahowald, N. M., Scanza, R., Brahney, J., Goodale, C. L., Hess, P. G., Moore, J. K., and Neff, J.: Aerosol Deposition
1002 Impacts on Land and Ocean Carbon Cycles, *Curr Clim Change Rep.*, 3, 16–31, <https://doi.org/10.1007/s40641-017-0056-z>, 2017.
- 1003
- 1004 Mahowald, N. M., Hamilton, D. S., Mackey, K. R. M., Moore, J. K., Baker, A. R., Scanza, R., and Zhang, Y.: Aerosol trace
1005 metal deposition dissolution and impacts on marine microorganisms and biogeochemistry, *Nature Communication*,
1006 81, 1–15, <https://doi.org/10.1038/s41467-018-04970-7>, 2018.
- 1007 Malm, W., Pitchford, M., McDade, C., and Ashbaugh, L.: Coarse particle speciation at selected locations in the rural
1008 continental United States, *Atmos Environ.*, 41, 225–2239, 2007.
- 1009 Mbengue, S., Zikova, N., Schwarz, J., Vodička, P., Šmejkalová, A. H., and Holoubek, I.: Mass absorption cross-section and
1010 absorption enhancement from long term black and elemental carbon measurements: A rural background station in
1011 Central Europe, *Science of the Total Environment*, 794, <https://doi.org/10.1016/j.scitotenv.2021.148365>, 2021.
- 1012 Marticorena, B., Chatenet, B., Rajot, J., Traore, S., Diallo, A., Kone, I., Maman, A., NDiaye, T., and Zakou, A.: Temporal
1013 variability of mineral dust concentrations over West Africa: analyses of a pluriannual monitoring from the AMMA
1014 Sahelian Dust Transect, *Atmos. Chem. Phys.*, 10, 2010–8899, 2010.
- 1015 Marticorena, B., Diallo, A., Rajot, J. L., Chatenet, B., Féron, A. , Gaimoz, C., Maisonneuve, F., Siour, G., Diop, T., and
1016 N'Diaye, T.: PM10 concentration, M'Bour, Senegal., Aeris, 2010.
- 1017 Matsui, H. and N. Mahowald (2017), Development of a global aerosol model using a two-dimensional sectional method: 2.
1018 Evaluation and sensitivity simulations, *Journal of Advances in Modeling Earth Systems*, 9, 1887-1920,
1019 doi:10.1002/2017MS000937.
- 1020 McNeill, J., Snider, G., Weagle, C. L., Walsh, B., Bissonnette, P., Stone, E., Abboud, I., Akoshile, C., Anh, N. X.,
1021 Balasubramanian, R., Brook, J. R., Coburn, C., Cohen, A., Dong, J., Gagnon, G., Garland, R. M., He, K., Holben,
1022 B. N., Kahn, R., Kim, J. S., Lagrosas, N., Lestari, P., Liu, Y., Jeba, F., Joy, K. S., Martins, J. V., Misra, A., Norford,
1023 L. K., Quel, E. J., Salam, A., Schichtel, B., Tripathi, S. N., Wang, C., Zhang, Q., Brauer, M., Gibson, M. D.,
1024 Rudich, Y., and Martin, R. V.: Large global variations in measured airborne metal concentrations driven by
1025 anthropogenic sources, *Sci Rep.*, 10, <https://doi.org/10.1038/s41598-020-78789-y>, 2020.
- 1026 Mihalopoulos N., E. Stephanou, M. Kanakidou, S. Pilitsidis and P. Bousquet, Tropospheric aerosol ionic composition above
1027 the Eastern Mediterranean Area, *Tellus B*, 49B, 314-326, 1997
- 1028 Mirante F., Oliveira C., Martins N., Pio C., Caseiro A., Cerqueira M., Alves C., Oliveira C., Oliveira J., Camões F., Matos
1029 M., and Silva H.: Carbonaceous content of atmospheric aerosols in Lisbon urban atmosphere. European
1030 Geophysical Union General Assembly, 2-7 May, Vienna, Austria, 2010.
- 1031 Mirante, F., Alves, C., Pio, C., Pindado, O., Perez, R., Revuelta, M. A., and Artiñano, B.: Organic composition of size
1032 segregated atmospheric particulate matter, during summer and winter sampling campaigns at representative sites in
1033 Madrid, Spain, *Atmos Res.*, 132–133, 345–361, <https://doi.org/10.1016/j.atmosres.2013.07.005>, 2013.



- 1034 1035 Mkoma, S. L.: Physico-chemical characterisation of atmospheric aerosols in Tanzania, with emphasis on the carbonaceous
aerosol components and on chemical mass closure, Ghent University, Ghent, Belgium, 2008.
- 1036 1037 Mkoma, S. L., Maenhaut, W., Chi, X., Wang, W., and Raes, N.: Characterisation of PM10 atmospheric aerosols for the wet
season 2005 at two sites in East Africa, *Atmos Environ*, 43, 631–639,
<https://doi.org/10.1016/j.atmosenv.2008.10.008>, 2009.
- 1038 1039 Morera-Gómez, Y., Elustondo, D., Lasheras, E., Alonso-Hernández, C. M., and Santamaría, J. M.: Chemical characterization
1040 of PM10 samples collected simultaneously at a rural and an urban site in the Caribbean coast: Local and long-range
1041 source apportionment, *Atmos Environ*, 192, 182–192, <https://doi.org/10.1016/j.atmosenv.2018.08.058>, 2018.
- 1042 1043 Morera-Gómez, Y., Santamaría, J. M., Elustondo, D., Lasheras, E., and Alonso-Hernández, C. M.: Determination and source
1044 apportionment of major and trace elements in atmospheric bulk deposition in a Caribbean rural area, *Atmos
Environ*, 202, 93–104, <https://doi.org/10.1016/j.atmosenv.2019.01.019>, 2019.
- 1045 1046 Mortier, A., Gliß, J., Schulz, M., Aas, W., Andrews, E., Bian, H., Chin, M., Ginoux, P., Hand, J., Holben, B., Zhang, H.,
Kipling, Z., Kirkevåg, A., Laj, P., Lurton, T., Myhre, G., Neubauer, D., Olivié, D., von Salzen, K., Skeie, R. B.,
1047 Takemura, T., and Tilmes, S.: Evaluation of climate model aerosol trends with ground-based observations over the
1048 last 2 decades - an AeroCom and CMIP6 analysis, *Atmos Chem Phys*, 20, 13355–13378,
<https://doi.org/10.5194/acp-20-13355-2020>, 2020.
- 1049 1050 Myriokefalakis S., Nenes A., Baker A.R., Mihalopoulos N., Kanakidou M.: Bioavailable atmospheric phosphorous supply
to the global ocean: a 3-D global modelling study, *Biogeosciences*, 13, 6519–6543, 2016,
www.biogeosciences.net/13/6519/2016/
- 1051 1052 1053 1054 Nava, S., Lucarelli, F., Amato, F., Becagli, S., Calzolai, G., Chiari, M., Giannoni, M., Traversi, R., and Udisti, R.: Biomass
burning contributions estimated by synergistic coupling of daily and hourly aerosol composition records, *Science of
the Total Environment*, 511, 11–20, <https://doi.org/10.1016/j.scitotenv.2014.11.034>, 2015.
- 1055 1056 1057 1058 Nava, S., Calzolai, G., Chiari, M., Giannoni, M., Giardi, F., Becagli, S., Severi, M., Traversi, R., and Lucarelli, F.: Source
apportionment of PM2.5 in Florence (Italy) by PMF analysis of aerosol composition records, *Atmosphere (Basel)*,
11, <https://doi.org/10.3390/ATMOS11050484>, 2020.
- 1059 1060 Neff, J., Reynolds, M. P., Munson, S., Fernandez, D., and Belnap, J.: The role of dust storms in total atmospheric particle
concentration at two sites in the western U.S., *J Geophys Res*, 118, 1–12, 2013.
- 1061 1062 1063 Nenes, A., Pandis, S. N., Kanakidou, M., Russell, A., Song, S., Vasilakos, P., and Weber, R. J.: Aerosol acidity and liquid
water content regulate the dry deposition of inorganic reactive nitrogen, *Atmos. Chem. Phys.*, 21, 6023–6033,
<https://doi.org/10.5194/acp-21-6023-2021>, 2021.
- 1064 1065 1066 Nyanganyura, D., Maenhaut, W., Mathutu, M., Makarau, A., and Meixner, F. X.: The chemical composition of tropospheric
aerosol particles and their contributing sources to a continental background site in northern Zimbabwe from 1994 to
2000, *Atmos. Environ.*, 41, 2644–2659, <https://doi.org/10.1016/j.atmosenv.2006.11.015>, 2007.



- 1067 Obiso, V., Gonçalves Ageitos, M., Pérez García-Pando,C., Schuster, G. L., Bauer, S. E., Di Biagio, C., Formenti, P.
1068 Perlitz, J. P., Tsigaridis,K., and Miller, R. L., 2023: Observationally constrained regional variations of shortwave
1069 absorption by iron oxides emphasize the cooling effect of dust. *Atmos. Chem. Phys.*, submitted.
1070 Oliveira, C., Pio, C., Caseiro, A., Santos, P., Nunes, T., Mao, H., Luhana, L., and Sokhi, R.: Road traffic impact on urban
1071 atmospheric aerosol loading at Oporto, Portugal, *Atmos Environ.*, 44, 3147–3158,
1072 <https://doi.org/10.1016/j.atmosenv.2010.05.027>, 2010.
1073 Oliveira C., PAHLIS Team: Atmospheric pollution in Lisbon urban atmosphere. European Geosciences Union General
1074 Assembly, 19-24 Apr., Vienna, Austria, 2009.
1075 Olson, J., Prather, M., Berntsen, T., Carmichael, G., Chatfield, R., Connell, P., Derwent, R., Horowitz, L., Jin, S.,
1076 Kanakidou, M., Kasibhatla, P., Kotamarthi, R., Kuhn, M., Law, K., Penner, J., Perliski, L., Sillman, S., Stordal, F.,
1077 Thompson, A., and Wild, O.: Results from the Intergovernmental Panel on Climatic Change Photochemical Model
1078 Intercomparison (PhotoComp), *Journal of Geophysical Research: Atmospheres*, 102, 5979–5991,
1079 <https://doi.org/doi:10.1029/96JD03380>, 1997.
1080 Paulot, F., Ginoux, P., Cooke, W. F., Donner, L. J., Fan, S., Lin, M. Y., Mao, J., Naik, V., and Horowitz, L. W.: Sensitivity
1081 of nitrate aerosols to ammonia emissions and to nitrate chemistry: Implications for present and future nitrate optical
1082 depth, *Atmos Chem Phys*, 16, 1459–1477, <https://doi.org/10.5194/acp-16-1459-2016>, 2016.
1083 Pérez, N., Pey, J., Querol, X., Alastuey, A., López, J. M., and Viana, M.: Partitioning of major and trace components in
1084 PM10-PM2.5-PM1 at an urban site in Southern Europe, *Atmos Environ.*, 42, 1677–1691,
1085 <https://doi.org/10.1016/j.atmosenv.2007.11.034>, 2008.
1086 Philip, S., Martin, R. v., Snider, G., Weagle, C. L., van Donkelaar, A., Brauer, M., Henze, D. K., Klimont, Z.,
1087 Venkataraman, C., Guttikunda, S. K., and Zhang, Q.: Anthropogenic fugitive, combustion and industrial dust is a
1088 significant, underrepresented fine particulate matter source in global atmospheric models, *Environmental Research
1089 Letters*, 12, 1–46, 2017.
1090 Pio, C., Rienda, I. C., Nunes, T., Gonçalves, C., Tchepel, O., Pina, N. K., Rodrigues, J., Lucarelli, F., and Alves, C. A.:
1091 Impact of biomass burning and non-exhaust vehicle emissions on PM10 levels in a mid-size non-industrial western
1092 Iberian city, *Atmos Environ.*, 289, <https://doi.org/10.1016/j.atmosenv.2022.119293>, 2022.
1093 Prank, M., Sofiev, M., Tsyró, S., Hendriks, C., Semeena, V., Francis, X. V., Butler, T., Van Der Gon, H. D., Friedrich, R.,
1094 Hendricks, J., Kong, X., Lawrence, M., Righi, M., Samaras, Z., Sausen, R., Kukkonen, J., and Sokhi, R.: Evaluation
1095 of the performance of four chemical transport models in predicting the aerosol chemical composition in Europe in
1096 2005, *Atmos Chem Phys*, 16, 6041–6070, <https://doi.org/10.5194/acp-16-6041-2016>, 2016.
1097 Prospero, J., Bullard, J., and Hodkins, R.: High-Latitude Dust Over the North Atlantic: Inputs from Icelandic Proglacial Dust
1098 Storms, *Science* (1979), 335, 1078–1082, 2012.



- 1099 Prospero, J., Barkely, A., Gaston, C., Gatineau, A., Campos y Sanasano, A., and Pulcherie, K. P.: Data From: Characterizing
1100 and quantifying African dust transport and deposition to South America: Implications for the phosphorus budget in
1101 the Amazon Basin, Miami, <https://doi.org/10.17604/vrsh-w974>, 2020.
- 1102 Prospero, J. M.: Long-range transport of mineral dust in the global atmosphere: Impact of African dust on the environment
1103 of the southeastern United States, Proc. Natl. Academy Science, 96, 3396–3403, 1999.
- 1104 Prospero, J. M., Uematsu, M., and Savoie, D. L.: Mineral Aerosol Transport to the Pacific Ocean, in: Chemical
1105 Oceanography, vol. 10, Academic Press Limited, 187–218, 1989.
- 1106 Prospero, J.: The atmospheric transport of particles to the ocean, in: Particle Flux in the Ocean, edited by: Ittekkot, I.,
1107 Schaffer, P., Honjo, S., and Depetris, P. J., John Wiley, New York, 1996.
- 1108 Prospero, J. M., Barrett, K., Church, T., Dentener, F., Duce, R. A., Galloway, J. N., Levy, H., Moody, J., and Quinn, P.:
1109 Atmospheric deposition of nutrients to the North Atlantic Basin, Biogeochemistry, 35, 27–73,
1110 <https://doi.org/10.1007/BF02179824>, 1996.
- 1111 Putaud, J.-P., Raes, F., Dingenen, R. Van, U. Baltensperger, Bruggemann, E., Facchini, M.-C., Decesari, S., Fuzzi, S., R.
1112 Gehrig, Huglin, C., Laj, P., Lorbeer, G., Maenhaut, W., N. Mihalopoulos, Muller, K., Querol, X., Rodriguez, S.,
1113 Schneider, J., G. Spindler, ten Brink, H., Torseth, K., and Wiedensohler, A.: A European aerosol phenomenology.
1114 2: chemical characteristics of particulate matter at kerbside, urban, rural and background sites in Europe, Atmos
1115 Environ, 38, 2579–2595, 2004.
- 1116 Putaud, J. P., Van Dingenen, R., Alastuey, A., Bauer, H., Birmili, W., Cyrys, J., Flentje, H., Fuzzi, S., Gehrig, R., Hansson,
1117 H. C., Harrison, R. M., Herrmann, H., Hitzenberger, R., Hüglin, C., Jones, A. M., Kasper-Giebl, A., Kiss, G.,
1118 Kousa, A., Kuhlbusch, T. A. J., Löschau, G., Maenhaut, W., Molnar, A., Moreno, T., Pekkanen, J., Perrino, C., Pitz,
1119 M., Puxbaum, H., Querol, X., Rodriguez, S., Salma, I., Schwarz, J., Smolik, J., Schneider, J., Spindler, G., ten
1120 Brink, H., Tursic, J., Viana, M., Wiedensohler, A., and Raes, F.: A European aerosol phenomenology - 3: Physical
1121 and chemical characteristics of particulate matter from 60 rural, urban, and kerbside sites across Europe, Atmos
1122 Environ, 44, 1308–1320, <https://doi.org/10.1016/j.atmosenv.2009.12.011>, 2010.
- 1123 Quaas, J., Jia, H., Smith, C., Albright, A. L., Aas, W., Bellouin, N., Boucher, O., Doutriaux-Boucher, M., Forster, P. M.,
1124 Grosvenor, D., Jenkins, S., Klimont, Z., Loeb, N. G., Ma, X., Naik, V., Paulot, F., Stier, P., Wild, M., Myhre, G., and Schulz,
1125 M.: Robust evidence for reversal of the trend in aerosol effective climate forcing, Atmos. Chem. Phys., 22, 12221–
1126 12239, <https://doi.org/10.5194/acp-22-12221-2022>, 2022.
- 1127 Rajot, J. L., Abdourhamane Touré, A. , Marticorena, B. , Bouet, C. , Chatenet, B. , Féron, A., Gaimoz, C. , Maisonneuve, F. ,
1128 Siour, G., Valorso, R. , Maman, A., and Zakou, A.: PM10 concentration, Banizoumbou, Niger. , Aeris., 2010a.
- 1129 Rajot, J. L. , Boubacar, A. , Marticorena, B. , Bouet, C. , Chatenet, B. , Féron, A. , Gaimoz, C. , Maisonneuve, F., Siour, G.,
1130 Valorso, R., Coulibaly, S. B. , Kouyaté, Z. , Coulibaly, B. , Coulibaly, M. , Koné, I., and Traoré, S.: PM10
1131 concentration, Cinzana, Mali., AERIS, 2010b.



- 1132 Regayre, L. A., Johnson, J. S., Yoshioka, M., Pringle, K. J., Sexton, D. M. H., Booth, B. B. B., Lee, L. A., Bellouin, N., and
1133 Carslaw, K. S.: Aerosol and physical atmosphere model parameters are both important sources of uncertainty in
1134 aerosol ERF, *Atmos Chem Phys*, 18, 9975–10006, <https://doi.org/10.5194/acp-18-9975-2018>, 2018.
- 1135 Reid, J. S., Jonson, H., Maring, H., Smirnov, A., Savoie, D., Cliff, S., Reid, E., Livingston, J., Meier, M., Dubovik, O., and
1136 Tsay, S.-C.: Comparison of size and morphological measurements of dust particles from Africa, *J Geophys Res*,
1137 108, 8593: doi:1029/2002JD002485, 2003.
- 1138 Remer, L., Kaufman, Y., Tanre, D., Mattoe, S., Chu, D., Martins, J., Li, R., Ichoku, C., Levy, R., Kleidman, R., Eck, T.,
1139 Vermote, E., and Holbren, B.: The MODIS aerosol algorithm, products and validation, *J Atmos Sci*, 62, 947–973,
1140 2005.
- 1141 Rodríguez, S., Alastuey, A., Alonso-Pérez, S., Querol, X., Cuevas, E., Abreu-Afonso, J., Viana, M., Pérez, N., Pandolfi, M.,
1142 and De La Rosa, J.: Transport of desert dust mixed with North African industrial pollutants in the subtropical
1143 Saharan Air Layer, *Atmos Chem Phys*, 11, 6663–6685, <https://doi.org/10.5194/acp-11-6663-2011>, 2011.
- 1144 Rodríguez, S., Alastuey, A., and Querol, X.: A review of methods for long term in situ characterization of aerosol dust,
1145 <https://doi.org/10.1016/j.aeolia.2012.07.004>, October 2012.
- 1146 Rodríguez, S., Cuevas, E., Prospero, J. M., Alastuey, A., Querol, X., López-Solano, J., García, M. I., and Alonso-Pérez, S.:
1147 Modulation of Saharan dust export by the North African dipole, *Atmos Chem Phys*, 15, 7471–7486,
1148 <https://doi.org/10.5194/acp-15-7471-2015>, 2015.
- 1149 Ryder, C. L., Highwood, E. J., Walser, A., Seibert, P., Philipp, A., and Weinzierl, B.: Coarse and giant particles are
1150 ubiquitous in Saharan dust export regions and are radiatively significant over the Sahara, *Atmos. Chem. Phys.*, 19,
1151 15353–15376, <https://doi.org/10.5194/acp-19-15353-2019>, 2019.
- 1152 Salma, I., Maenhaut, W., Annegarn, H. J., Andreae, M. O., Meixner, F. X., and Garstang, M.: Combined application of
1153 INAA and PIXE for studying the regional aerosol composition in Southern Africa, *Journal of Geophysical
1154 Research*, 101, 2361–23650, 1997.
- 1155 Savoie, D. L., Prospero, J. M., Larsen, R. J., Huang, R., Izaguirre, M. A., Huang, T., Snowdon, T., Custals, L., and
1156 Sanderson, C.: Nitrogen and sulfur species in Antarctic aerosols at Mawson, Palmer Station, and Marsh (King
1157 George Island), *J Atmos Chem*, 17, 95–122, 1993.
- 1158 Scanza, R., Mahowald, N., Ghan, S., Zender, C., Kok, J., Liu, X., and Zhang, Y.: Dependence of dust radiative forcing on
1159 mineralogy in the Community Atmosphere Model, *Atmos Chem Phys*, 15, 537–561, 2015.
- 1160 Schulz, M., Textor, C., Kinne, S., Balkanski, Y., Bauer, S., Berntsen, T., Berglen, T., Boucher, O., Dentener, F., Guibert, S.,
1161 Isaksen, I. S. A., Iversen, T., Koch, D., Kirkevåg, A., Liu, X., Montanaro, V., Myhre, G., Penner, J. E., Pitari, G.,
1162 Reddy, S.,
- 1163 Schuster, G. L., Dubovik, O., and Arola, A.: Remote sensing of soot carbon – Part 1: Distinguishing different absorbing
1164 aerosol species, *Atmos. Chem. Phys.*, 16, 1565–1585, <https://doi.org/10.5194/acp-16-1565-2016>, 2016.



- 1165 Seland, Ø., Stier, P., and Takemura, T.: Radiative forcing by aerosols as derived from the AeroCom present-day and
1166 preindustrial simulations, *Atmos Chem Phys*, 6, 2006–5225, 2006.
- 1167 Schutgens, N. A. J., Gryspeerdt, E., Weigum, N., Tsyro, S., Goto, D., Schulz, M., and Stier, P.: Will a perfect model agree
1168 with perfect observations? The impact of spatial sampling, *Atmos Chem Phys*, 16, 6335–6353,
1169 <https://doi.org/10.5194/acp-16-6335-2016>, 2016.
- 1170 Seinfeld, J. and Pandis, S.: *Atmospheric Chemistry and Physics*, John Wiley and Sons, Inc, New York, 1326 pp., 1998.
- 1171 Seinfeld, J. H. and Pandis, S. N.: *Atmospheric Chemistry and Physics: From Air Pollution to Climate Change*, 2006.
- 1172 Silva, H.F., Matos, M. J., Oliveira, C., Ferreira, A. F., Oliveira, J. C., Cantinho, P., Calado, M., Oliveira, C., Martins, N., Pio,
1173 C., and Camões M. F. : Effect of climate on PM concentration and size distribution in two sites in the city of
1174 Lisbon, Encontro de Jovens Químicos Portugueses, Aveiro, 21 to 23 of April, 2010.
- 1175 Skiles, S. M. K., Flanner, M., Cook, J. M., Dumont, M., and Painter, T. H.: Radiative forcing by light-absorbing particles in
1176 snow, <https://doi.org/10.1038/s41558-018-0296-5>, 1 November 2018.
- 1177 Smichowski, P., Gómez, D. R., Dawidowski, L. E., Giné, M. F., Bellato, A. C. S., and Reich, S. L.: Monitoring trace metals
1178 in urban aerosols from Buenos Aires city. Determination by plasma-based techniques, *Journal of Environmental
1179 Monitoring*, 6, 286–294, <https://doi.org/10.1039/b312446k>, 2004.
- 1180 Swap, R., Garstang, M., Greco, S., Talbot, R., and Kallberg, P.: Saharan dust in the Amazon Basin, *Tellus*, 44B, 133–149,
1181 <https://doi.org/https://doi.org/10.3402/tellusb.v44i2.15434>, 1992.
- 1182 Szopa, S., Naik, V., Adhikary, B., Artaxo, P., Berntsen, T., Collins, W. D., Aas, W., Akritidis, D., Allen, R. J., Kanaya, Y.,
1183 Prather, M. J., Kuo, C., Zhai, P., Pirani, A., Connors, S., Péan, C., Berger, S., Caud, N., Chen, Y., Goldfarb, L.,
1184 Gomis, M., Huang, M., Leitzell, K., Lonnoy, E., Matthews, J., Maycock, T., Waterfield, T., Yelekçi, O., Yu, R., and
1185 Zhou, B.: Chapter 6: Short-lived Climate Forcers, in: *Climate Change 2021: The Physical Science Basis.*
1186 Contribution of Working Group I to the Sixth Assessment Report of the Intergovernmental Panel on Climate
1187 Change, edited by: Masson-Delmotte, V. , Zhai, P., A. Pirani, A., Connors, S. L., Péan, C. S., Berger, S., Caud, N.,
1188 Chen, Y., Goldfarb, L., Gomis, M. I., Huang, M., Leitzell, K., Lonnoy, E., Matthews, J. B. R., Maycock, T. K.,
1189 Waterfield, T., Yelekçi, O., Yu, R., and Zhou, B., Cambridge University Press, , Cambridge, United Kingdom and
1190 New York, NY, USA, 816–921, <https://doi.org/10.1017/9781009157896.008>, 2021.
- 1191 Tanré, D., Kaufman, Y. J., Herman, M., and Mattoo, S.: Remote sensing of aerosol properties over oceans using the
1192 MODIS/EOS spectral radiances, *J Geophys Res*, 102, 16,916-971,988, 1997.
- 1193 Textor, C. and others: Analysis and quantification of the diversities of aerosol life cycles within AeroCOM, *Atmos Chem
1194 Phys*, 6, 1777–1813, 2006.
- 1195 Thornhill, G., Collins, W., Olivié, D., Archibald, A., Bauer, S., Checa-Garcia, R., Fiedler, S., Folberth, G., Gjermundsen, A.,
1196 Horowitz, L., Lamarque, J.-F., Michou, M., Mulcahy, J., Nabat, P., Naik, V., O'Connor, F., Paulot, F., Schulz, M.,
1197 Scott, C., Seferian, R., Smith, C., Takemura, T., Tilmes, S., and Weber, J.: Climate-driven chemistry and aerosol
1198 feedbacks in CMIP6 Earth system models, *Atmos Chem Phys*, 1–36, <https://doi.org/10.5194/acp-2019-1207>, 2020.



- 1199 Thornhill, G., Collins, W., Olivié, D., B. Skeie, R., Archibald, A., Bauer, S., Checa-Garcia, R., Fiedler, S., Folberth, G.,
1200 Gjermundsen, A., Horowitz, L., Lamarque, J. F., Michou, M., Mulcahy, J., Nabat, P., Naik, V., M. O'Connor, F.,
1201 Paulot, F., Schulz, M., E. Scott, C., Séférian, R., Smith, C., Takemura, T., Tilmes, S., Tsigaridis, K., and Weber, J.:
1202 Climate-driven chemistry and aerosol feedbacks in CMIP6 Earth system models, *Atmos Chem Phys*, 21, 1105–
1203 1126, <https://doi.org/10.5194/acp-21-1105-2021>, 2021.
1204 Tørseth, K., Aas, W., Breivik, K., Fjeraa, A. M., Fiebig, M., Hjellbrekke, A. G., Lund Myhre, C., Solberg, S., and Yttri, K. E.:
1205 Introduction to the European Monitoring and Evaluation Programme (EMEP) and observed atmospheric composition
1206 change during 1972–2009, <https://doi.org/10.5194/acp-12-5447-2012>, 2012.
1207 Tsigaridis K., N. Daskalakis, M. Kanakidou, P. J. Adams, P. Artaxo, R. Bahadur, Y. Balkanski, S. E. Bauer, N. Bellouin, A.
1208 Benedetti, T. Bergman, T. K. Berntsen, J. P. Beukes, H. Bian, K. S. Carslaw, M. Chin, G. Curci, T. Diehl, R. C.
1209 Easter, S. J. Ghan, S. L. Gong, A. Hodzic, C. R. Hoyle, T. Iversen, S. Jathar, J. L. Jimenez, J. W. Kaiser, A. Kirkevag,
1210 D. Koch, H. Kokkola, Y. H Lee, G. Lin, X. Liu, G. Luo, X. Ma, G. W. Mann, N. Mihalopoulos, J.-J. Morcrette, J.-F.
1211 Muller, G. Myhre, S. Myrookefalitakis, N. L. Ng, D. O'Donnell, J. E. Penner, L. Pozzoli, K. J. Pringle, L. M. Russell,
1212 M. Schulz, J. Sciare, O. Seland, D. T. Shindell, S. Sillman, R. B. Skeie, D. Spracklen, T. Stavrakou, S. D. Steenrod,
1213 T. Takemura, P. Tiitta, S. Tilmes, H. Tost, T. van Noije, P. G. van Zyl, K. von Salzen, F. Yu, Z. Wang, Z. Wang, R.
1214 A. Zaveri, H. Zhang, K. Zhang, Q. Zhang, and X. Zhang, The AeroCom evaluation and intercomparison of organic
1215 aerosol in global models, *Atmospheric Chemistry and Physics*, 14, pp. 10845–10895, 2014.
1216 Uematsu, M., Duce, R. A., Prospero, J. M., Chen, L., Merrill, J. T., and McDonald, R. L.: Transport of Mineral Aerosol
1217 From Asia Over the North Pacific Ocean, *J Geophys Res*, 88, 5343–5352, 1983.
1218 Van Donkelaar, A., Hammer, M. S., Bindle, L., Brauer, M., Brook, J. R., Garay, M. J., Hsu, N. C., Kalashnikova, O. V.,
1219 Kahn, R. A., Lee, C., Levy, R. C., Lyapustin, A., Sayer, A. M., and Martin, R. V.: Monthly Global Estimates of
1220 Fine Particulate Matter and Their Uncertainty, *Environ Sci Technol*, 55, 15287–15300,
1221 <https://doi.org/10.1021/acs.est.1c05309>, 2021.
1222 Vanderzalm, J. L., Hooper, M. A., Ryan, B., Maenhaut, W., P. Martin, P. R., Rayment, and Hooper, B. M.: Impact of
1223 seasonal biomass burning on air quality in the “Top End” of regional northern Australia, *Clean Air Environ.*
1224 Qual., 37, 28–34, 2003.
1225 Vet, R., Artz, R. S. R. S., Carou, S., Shaw, M., Ro, C.-U. C.-U., Aas, W., Baker, A., Bowersox, V. C., Dentener, F., Galy-
1226 Lacaux, C., Hou, A., Pienaar, J. J., Gillett, R., Forti, M. C. C., Gromov, S., Hara, H., Khodzher, T., Mahowald, N.
1227 M. N. M., Nickovic, S., Rao, P. S. P., Reid, N. W. N. W., Dentener, F., Galy-Lacaux, C., Hou, A., Gillett, R., Forti,
1228 M. C. C., Gromov, S., Hara, H., Khodzher, T., Mahowald, N. M. N. M., Nickovic, S., Reid, N. W. N. W., Vet, R.,
1229 Artz, R. S., Carou, S., Shaw, M., Ro, C.-U., Aas, W., Baker, A., Bowersox, V. C., Dentener, F., Galy-Lacaux, C.,
1230 Hou, A., Pienaar, J. J., Gillett, R., Forti, M. C., Gromov, S., Hara, H., Khodzher, T., Mahowald, N. M., Nickovic,
1231 S., Rao, P. S. P., and Reid, N. W. N. W.: A global assessment of precipitation chemistry and depositioin of sulfur,



- 1232 nitrogen, sea salt , base cations, organic acids, acidity and pH and phosphorus, Atmospheric Enviroment, 93, 3–100,
1233 2014.
- 1234 Vira, J., Hess, P., Melkonian, J., and Wieder, W. R.: An improved mechanistic model for ammonia volatilization in Earth
1235 system models: Flow of Agricultural Nitrogen version 2 (FANv2), Geosci Model Dev, 13, 4459–4490,
1236 <https://doi.org/10.5194/gmd-13-4459-2020>, 2020.
- 1237 Vira, J., Hess, P., Ossohou, M., and Galy-Lacaux, C.: Evaluation of interactive and prescribed agricultural ammonia
1238 emissions for simulating atmospheric composition in CAM-chem, Atmos Chem Phys, 22, 1883–1904,
1239 <https://doi.org/10.5194/acp-22-1883-2022>, 2022.
- 1240 Virkkula, A., Aurela, M., Hillamo, R., Makela, T., Pakkanen, T., Kerminen, V. M., Maenhaut, W., Francois, F., and
1241 Cafmeyer, J.: Chemical composition of atmospheric aerosol in the European subarctic: Contribution of the Kola
1242 Peninsula smelter areas, central Europe and the Arctic Ocean, Journal Geophysical Research, 104, 23,681–23,696,
1243 <https://doi.org/10.1029/1999JD900426>, 1999.
- 1244 Webb, N. P. and Pierre, C.: Quantifying Anthropogenic Dust Emissions, Earths Future, 6, 286–295,
1245 <https://doi.org/10.1002/2017EF000766>, 2018.
- 1246 Wilson, W. E., Chow, J. C., Claiborn, C., Fusheng, W., Engelbrecht, J., and Watson, J. G.: Monitoring of particulate matter
1247 outdoors, 1009–1043 pp., 2002.
- 1248 Xiao, Y. H., Liu, S. R., Tong, F. C., Kuang, Y. W., Chen, B. F., and Guo, Y. D.: Characteristics and sources of metals in
1249 TSP and PM2.5 in an urban forest park at Guangzhou, Atmosphere (Basel), 5, 775–787,
1250 <https://doi.org/10.3390/atmos5040775>, 2014.
- 1251 Xu, L. and Penner, J. E.: Global simulations of nitrate and ammonium aerosols and their radiative effects, Atmos Chem
1252 Phys, 12, 9479–9504, <https://doi.org/10.5194/acp-12-9479-2012>, 2012.
- 1253 Yang, Y., Wang, H., Smith, S. J., Zhang, R., Lou, S., Yu, H., Li, C., and Rasch, P. J.: Source Apportionments of Aerosols
1254 and Their Direct Radiative Forcing and Long-Term Trends Over Continental United States, Earths Future, 6, 793–
1255 808, <https://doi.org/10.1029/2018EF000859>, 2018.
- 1256 Zender, C., Bian, H., and Newman, D.: Mineral Dust Entrainment and Deposition (DEAD) model: Description and 1990s
1257 dust climatology, J Geophys Res, 108, 4416, doi:10.1029/2002JD002775, 2003.
- 1258 Zhang, Y., Mahowald, N., Scanza, R. A., Journet, E., Desboeufs, K., Albani, S., Kok, J. F., Zhuang, G., Chen, Y., Cohen, D.
1259 D., Paytan, A., Patey, M. D., Achterberg, E. P., Engelbrecht, J. P., and Fomba, K. W.: Modeling the global
1260 emission, transport and deposition of trace elements associated with mineral dust, Biogeosciences, 12,
1261 <https://doi.org/10.5194/bg-12-5771-2015>, 2015.
- 1262 Zhao, A., Ryder, C. L., and Wilcox, L. J.: How well do the CMIP6 models simulate dust aerosols?, Atmos Chem Phys, 22,
1263 2095–2119, <https://doi.org/10.5194/acp-22-2095-2022>, 2022.



- 1264 Zhao, X., Liu, X., Burrows, S. M., and Shi, Y.: Effects of marine organic aerosols as sources of immersion-mode ice-
1265 nucleating particles on high-latitude mixed-phase clouds, *Atmos Chem Phys*, 21, 2305–2327,
1266 <https://doi.org/10.5194/acp-21-2305-2021>, 2021.
1267 Zihan, Q. and Losno, R.: Chemical properties of continental aerosol transported over the Southern Ocean: Patagonian and
1268 Namibian sources, Paris, France, 215 pp., 2016.
1269
1270

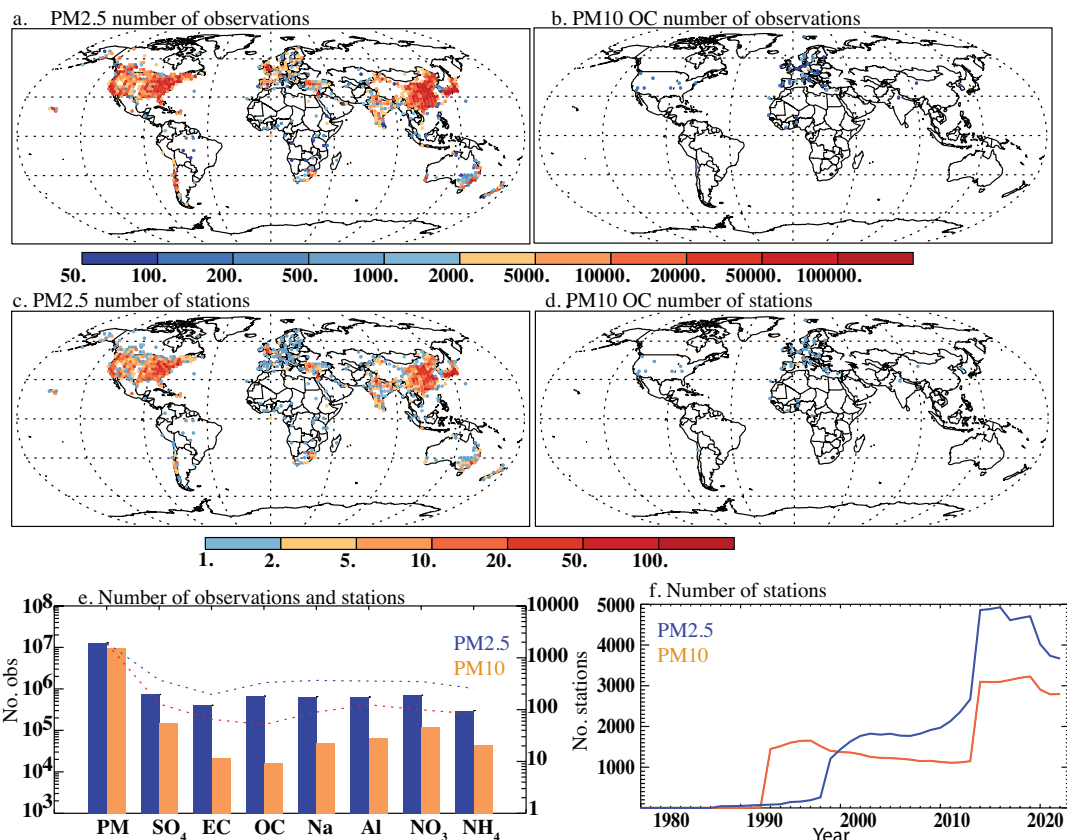


Figure 1: Distribution of observations in the data base, showing the number of observations of $\text{PM}_{2.5}$ (a) and PM_{10} Organic carbon (OC) (b) (with the colors indicating different numbers using the top color bar), as well as the number of stations within each 2×2 grid locations for $\text{PM}_{2.5}$ (c) and PM_{10} OC (d) (using the second color bar), showing that there is much more $\text{PM}_{2.5}$ or PM_{10} data, in contrast to speciated data. e) The number of observations (bars) for total particulate matter (PM) or speciated data is summarized in for the $\text{PM}_{2.5}$ (blue) and PM_{10} (orange) fraction using the left hand side y-axis. The number of stations included in the study for each 2×2 grid box is shown as a dotted line (e) and uses the right hand size y-axis. f) The number of stations of $\text{PM}_{2.5}$ (blue) and PM_{10} (orange) for each year is shown. The stations included derive from the following sources (see supplemental dataset for more details): (Alastuey et al., 2016; Almeida et al., 2005; Amato et al., 2016; Andreae et al., 2002; Arimoto et al., 2003; Artaxo et al., 2002; Barkley et al., 2019; Barraza et al., 2017; Bergametti et al., 1989; Bouet et al., 2019; 2021; Bozlaker et al., 2013; Chen et al., 2006; Chuang et al., 2005; Cipoli et al., 2023; Cohen et al., 2004; da Silva et al., 2008; Dongarrà et al., 2007, 2010; Formenti et al., 2003; Fuzzi et al., 2007; Hand et al., 2017; Heimbürger et al., 2012; Herut and Krom, 1996; Herut et al., 2001; Hsu et al., 2016; Hueglin et al., 2005;



Furu et al., 2022, 2015; Gianini et al., 2012a, b; Kalivitis et al., 2007; Kaly et al., 2015; Kubilay et al., 2000; Kyllönen et al., 2020; Laing et al., 2014b, a; Lucarelli et al., 2014; 2019; Mackey et al., 2013; Maenhaut et al., 1996c, a, b, 1997a, b; 1999, 2000a, 2000b, 2002a,b,2005;, 2008, 2011; Maenhaut and Cafmeyer, 1998; Malm et al., 2007; Marticorena et al., 2010; Mihalopoulos et al., 1997; Mirante et al., 2009, 2013; Mkoma, 2008, 2009; Morera-Gómez et al., 2018, 2019; Nava et al., 2015, 2020; Nyanganyura et al., 2007; Oliveira et al., 2009, 2010; Pérez et al., 2008; Pio et al., 2023; Prospero et al., 1989, 2012, 2020; Prospero, 1996, 1999; Putaud et al., 2004, 2010; Rajot et al., 2010a, 2010b; Rodríguez et al., 2011, 2015; Salma et al., 1997; Savoie et al., 1993; Silva et al., 2010; Smichowski et al., 2004; Swap et al., 1992; Tørseth et al., 2012; Uematsu et al., 1983; Vanderzalm et al., 2003; Virkkula et al., 1999; Xiao et al., 2014; Zihan and Losno, 2016. Data from several online networks are also included (see Supplemental dataset for more details): e.g. <https://www.airnow.gov/international/us-embassies-and-consulates/>, <https://quotsoft.net/air/>, <https://app.cpcbccr.com/cer/#/caaqm-dashboard-all/caaqm-landing/data>, <https://sinca.mma.gob.cl/index.php/>. <https://tenbou.nies.go.jp/download/>

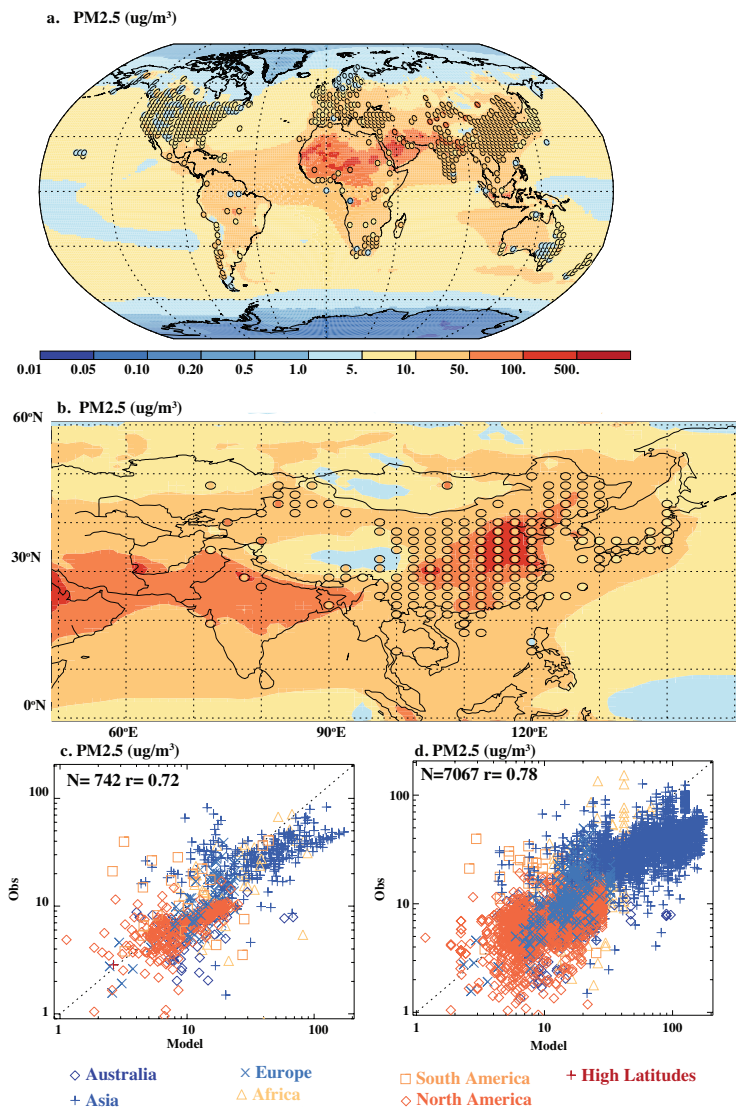


Figure 2: Model results and gridded observations for $\text{PM}_{2.5}$ in $\mu\text{g}/\text{m}^3$ spatially mapped globally (a) and focused on just East Asia (b) where the model is plotted as the background and the observations are circles with the colors indicating the amount of $\text{PM}_{2.5}$ using the same scale. A comparison of the model (x-axis) to the observations (y-axis) is shown for the gridded data (c) and including all stations (d). In the scatter plots, the colors and symbols indicate the regions. More statistics are shown in Table S4, and the model plotted alone is available in Figure S2.

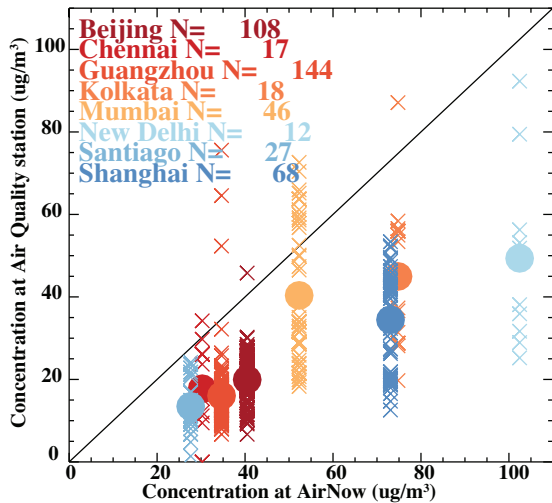
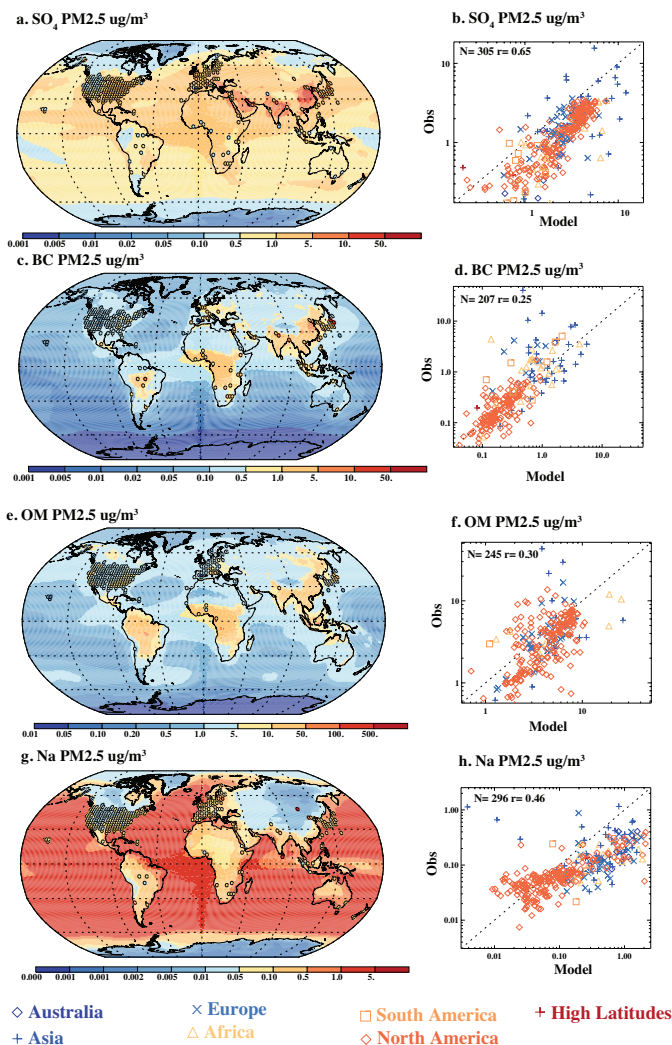


Figure 3: Comparison of PM_{2.5} observations from the US Embassy's AirNow network (<https://www.airnow.gov/international/us-embassies-and-consulates/>) versus observations from the Chinese air quality network (downloaded from <https://quotsoft.net/air/>) (Beijing 39.9N 116.4E, Guangzhou 23N 113E, Shanghai 31N 121E) and the Indian (Chennai 13N 80E, Kolkata 23N 88E, New Delhi 27N 77E) network (<https://app.cpcbccr.com/cer/#/caaqm-dashboard-all/caaqm-landing/data>); and observations (Barraza et al., 2017) from Santiago, Chile (23.7S 70.4W) against the Chilean air quality network (<https://sinca.mma.gob.cl/index.php/>). The numbers after each city name are the number of stations found within 1° distance of the AirNow (or Chile observations) station.



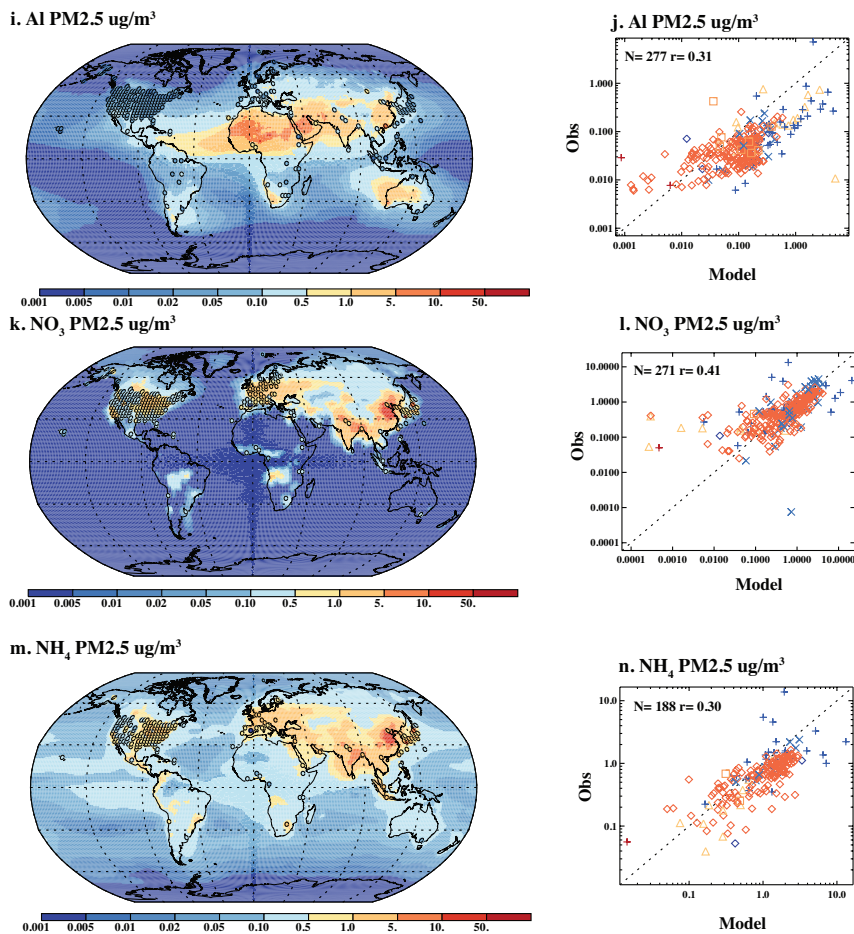


Figure 4: Model results and gridded observations for different types of PM_{2.5} in $\mu\text{g}/\text{m}^3$ spatially mapped globally where the model is plotted as the background and the observations are circles with the colors indicating the amount PM_{2.5} using the same scale for (a) SO₄²⁻, (c) BC (black carbon), (e) OM (organic material=1.8 times organic carbon (OC)), (g) Na, (i) Al, (k) NO₃⁻, (m) NH₄⁺. A scatter plot comparison of the model (x-axis) to the observations (y-axis) is shown for the gridded observational data for for (b) SO₄²⁻, (d) BC (f) OM, (h) Na, (j) Al, (l) NO₃⁻, (n) NH₄⁺. In the scatter plots, the colors and symbols indicate the regions using the same legend as Figure 2. More statistics are shown in Table S4, and the model plotted alone is available in Figure S2.

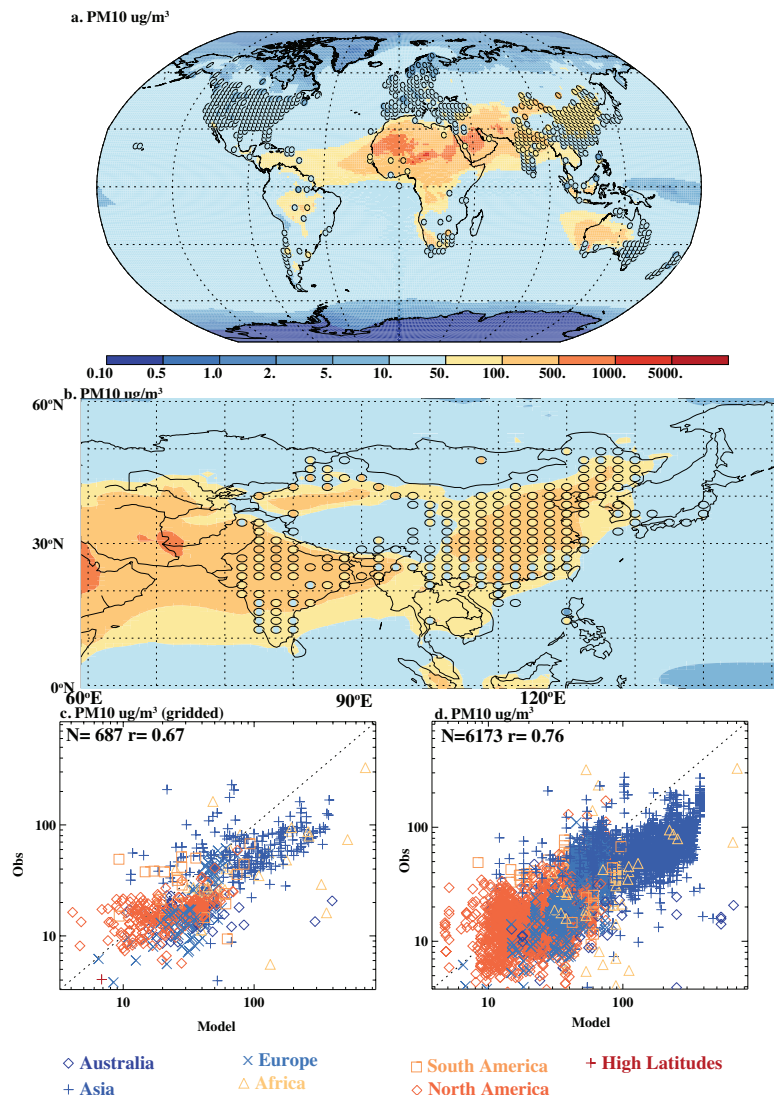
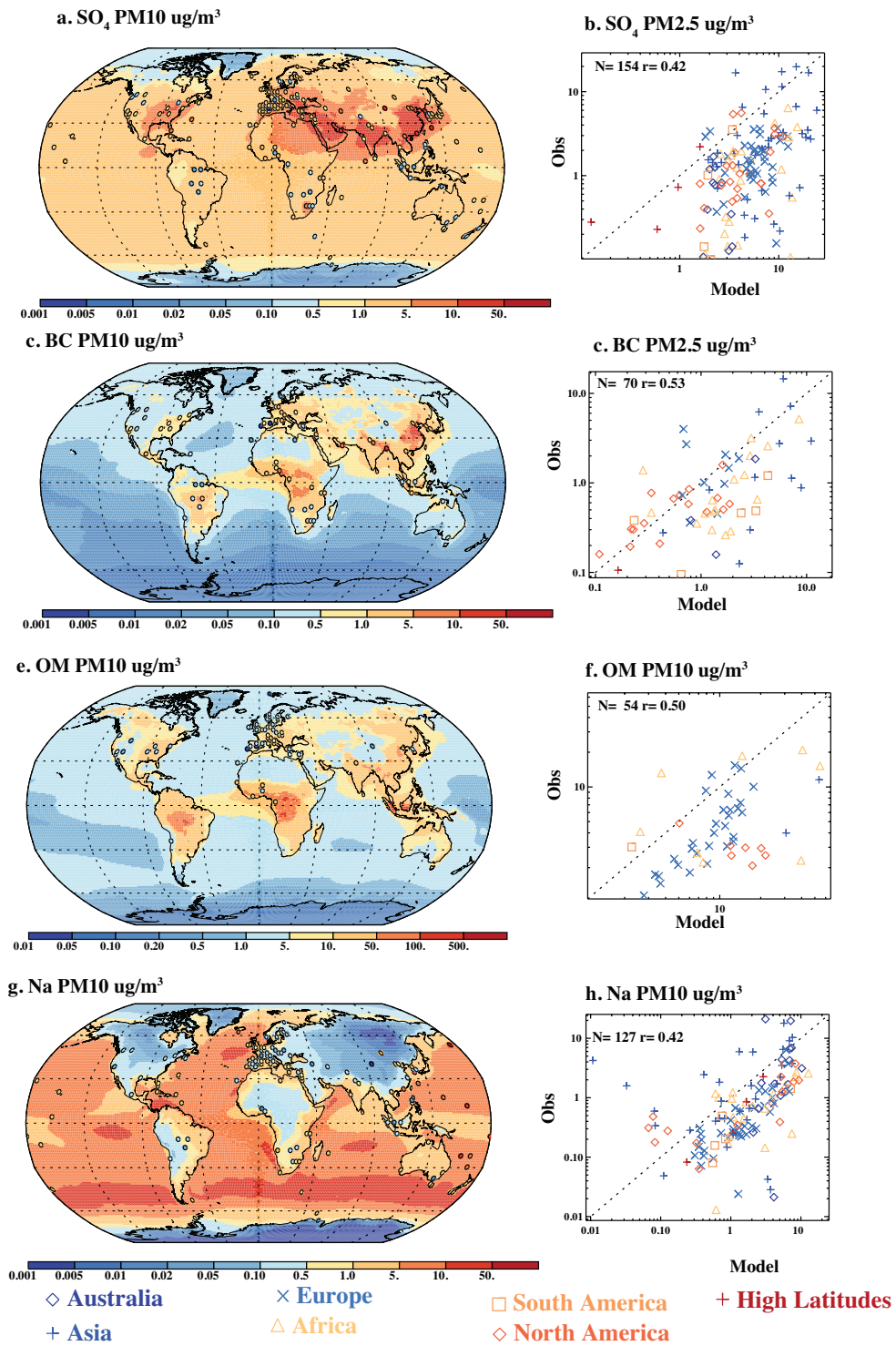


Figure 5: Model results and gridded observations for PM₁₀ in $\mu\text{g}/\text{m}^3$ spatially mapped globally (a) and focused on just East Asia (b) where the model is plotted as the background and the observations are circles with the colors indicating the amount of PM_{2.5} using the same scale. A comparison of the model (x-axis) to the observations (y-axis) is shown for the gridded data (c) and including all stations (d). In the scatter plots, the colors and symbols indicate the regions. More statistics are shown in Table S5, and the model plotted alone is available in Figure S3.



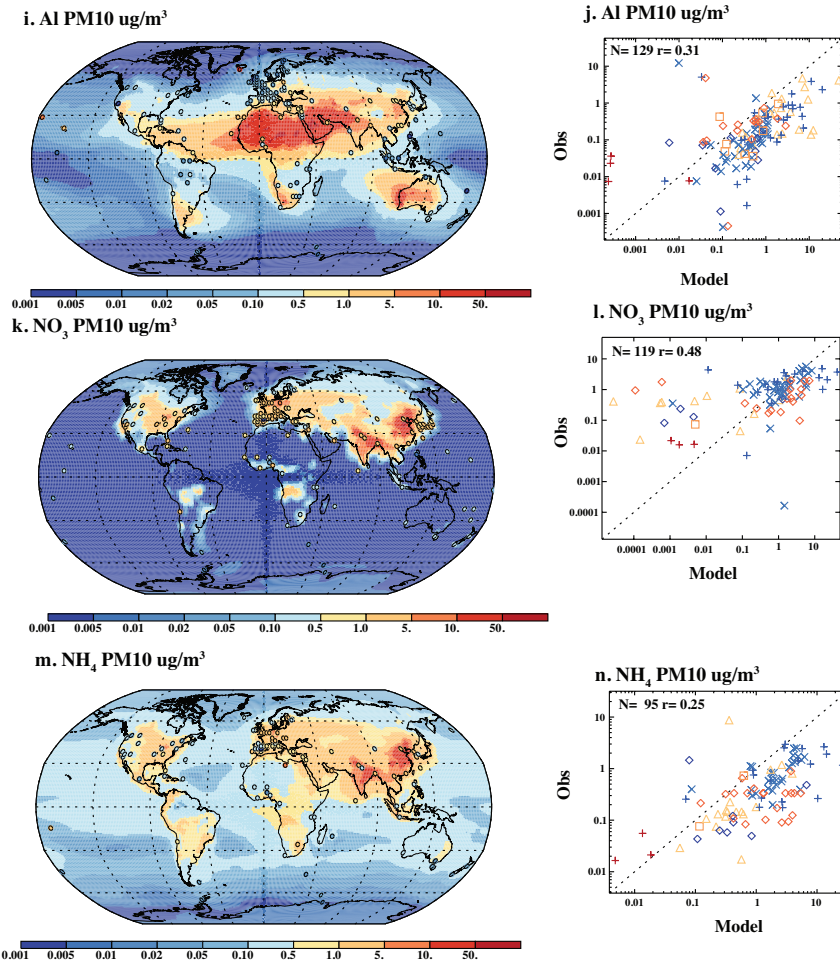
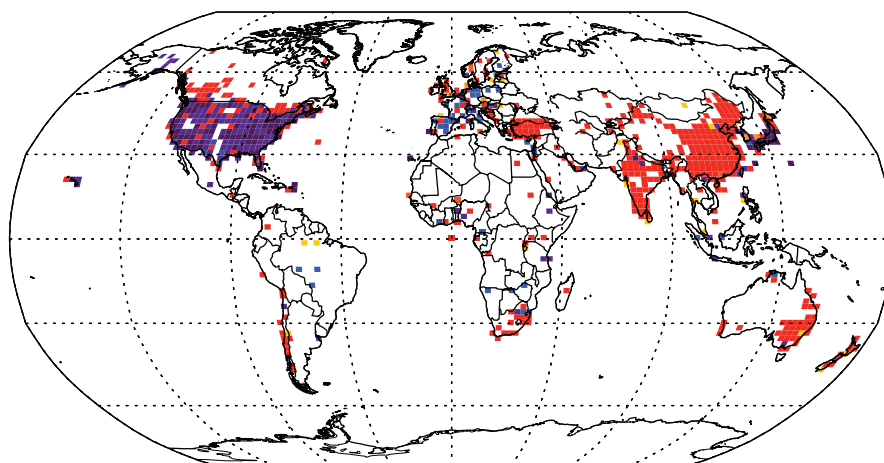


Figure 6: Model results and gridded observations for different types of PM₁₀ in $\mu\text{g}/\text{m}^3$ spatially mapped globally where the model is plotted as the background and the observations are circles with the colors indicating the amount PM₁₀ using the same scale for (a) SO₄²⁻, (c) BC (black carbon), (e) OM (organic material=1.8times organic carbon (OC)), (g) Na, (i) Al, (k) NO₃⁻, (m) NH₄⁺. A scatter plot comparison of the model (x-axis) to the observations (y-axis) is shown for the gridded observational data for (b) SO₄²⁻, (d) BC (f) OM, (h) Na, (j) Al, (l) NO₃⁻, (n) NH₄⁺. In the scatter plots, the colors and symbols indicate the regions using the same legend as Figure 2. More statistics are shown in Table S5, and the model plotted alone is available in Figure S3.



a. PM_{2.5} coverage (%)



b. PM₁₀ coverage (%)

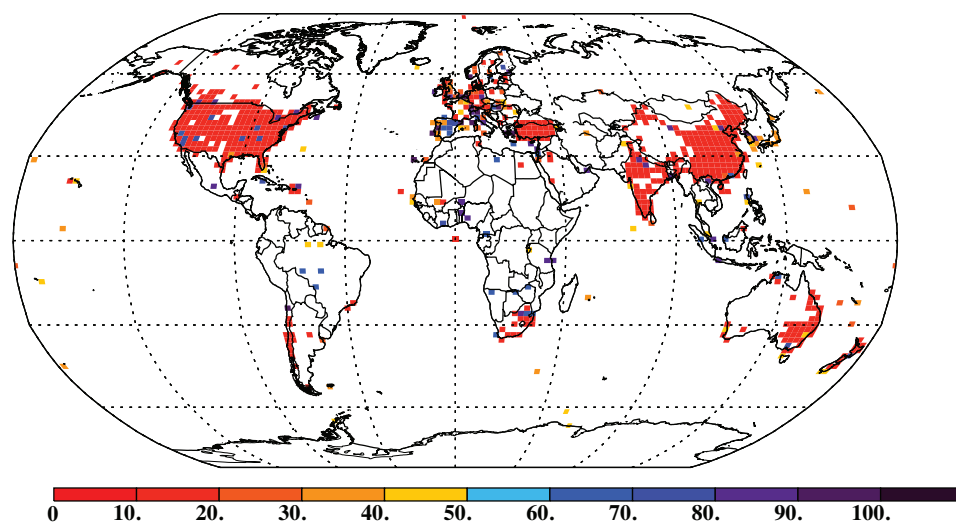


Figure 7: Observational coverage (%) for gridded observations, showing within each grid box (2x2) the % of the constituents that are measured assuming that PM, SO₄²⁻, BC, OM, Na, Al, NO₃⁻, and NH₄⁺ are required to constrain the PM distribution for (a) PM_{2.5} and (b) PM₁₀.

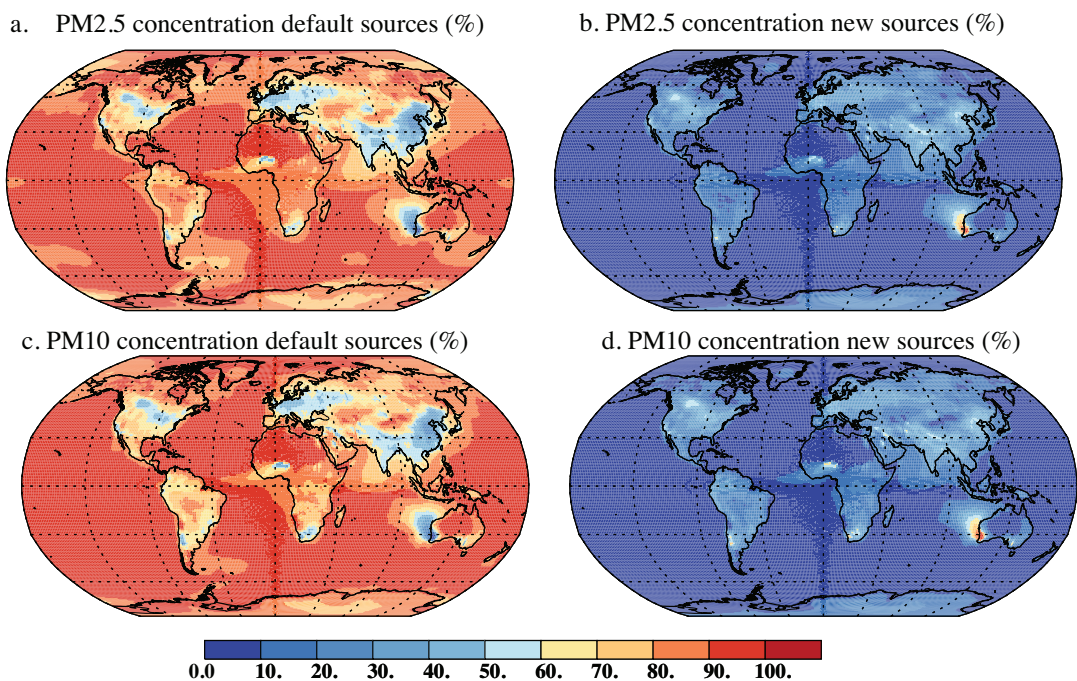


Figure 8: Modelled estimates of what percent of the surface concentration of PM_{2.5} is considered in the default CAM (a) or is new in this study (b). Similarly PM₁₀ is shown for the default model (c) and new sources in this study (d).



Table 1: Global Aerosol Budgets

Global deposition (Tg/year), percentage of aerosol that is PM_{2.5}, and globally and annually averaged surface concentration ($\mu\text{g}/\text{m}^3$) and aerosol optical depth for each of the sources used in the model. An asterisk indicates that there are additions to the model from the default CAM6.

	PM ₁₀	PM _{2.5}	Conc ($\mu\text{g}/\text{m}^3$)	AOD (unitless)
Sulfate	121	100	2.1	0.018
Black carbon	10	100	0.5	0.009
Primary organic aerosol	34	100	1.6	0.008
Secondary organic aerosol	37	100	1.0	0.007
Sea salts	2520	3	13.0	0.045
Dust	2870	1	19.4	0.030
NH ₄ NO ₃ *	20	100	0.4	0.013
Agricultural Dust*	585	1	3.7	0.006
Road*	0.43	79	0.02	0.0000
Coarse organic carbon*	4	0.0	0.04	0.0000
Coarse black carbon*	0.35	0.0	0.00	0.0000
Fine and coarse inorganic industrial matter *	56	46	1.2	0.0018
Bacteria and Fungi spores from land*	4	0	0.04	0.0000
Other primary biogenic	54	3	0.4	0.0005



particles from land*				
Marine organic aerosols	44	99	0.6	0.0008